Techniques for CG Music Video Production: the making of *Dance to the Music / Play to the Motion*

Adriana Schulz
Marcelo Cicconet
Bruno Madeira
Aldo Zang
Luiz Velho

VISGRAF Laboratory

March 2010

Abstract

This technical report presents a set of techniques for the production of music videos using computer graphics and animation. Their practical application is illustrated through examples developed for making the video “Dance to the Music / Play to the Motion”.

Contents

Chapter 1

Introduction

In this document we will present the making of "Dance to the Music / Play to the Motion" music video. The main motivation to write this technical report is to introduce through practical examples the basic set of computer graphics and animation techniques that are commonly used to create special effects and produce artistic videos.

1.1 The Video

Overview

The Dance to the Music / Play to the Motion piece was produced as part of a research project of the VISGRAF Laboratory on the areas of Computer Animation and Music. Its purpose was to test various methods being developed in our current research and to validate their effectiveness in the context of a real application.

The video combines novel aspects of automatic music composition with computer generated animation and high quality rendering to investigate an authoring paradigm for expressive audio-visual content creation.

Essentially the project tries to answer the following question: *"Is it possible to use dance in order to compose music"* ? For this purpose, we employed motion analysis techniques to drive a song synthesis probabilistic machine, such that the choreographed movements of a real dancer create new music that is subsequently performed by a computer animated character.

Storyboard

To demonstrate the results of the project a video was produced showing all the steps of this process.

We wanted the video to be, at the same time, artistic and illustrative – an authoring decision that posed great challenges to us.

The strategy adopted to fulfill our goal was to make the video more like a dance performance in itself than a documentary explaining the inner workings of the research. On the other hand, the video should also reveal the interplay of music and dance to produce an integrated piece.

Consequently, the structure of the narrative consisted of a dancer performing a samba song. This performance is divided in two parts: in the first part, she dances to an automatic generated music; and in the second part, the real dancer becomes a virtual dancer that, through her movements, create a new music. In other words, the paradigm: Dance to The Music / Play to the Motion.

Hints of how some technical aspects of the method relate to the actual action are provided by text explanations at both begining and end of the video, as well as, by graphical elements, such diagrams that are superimposed on the images throughout the video. The figure below shows the storyboard for this video:

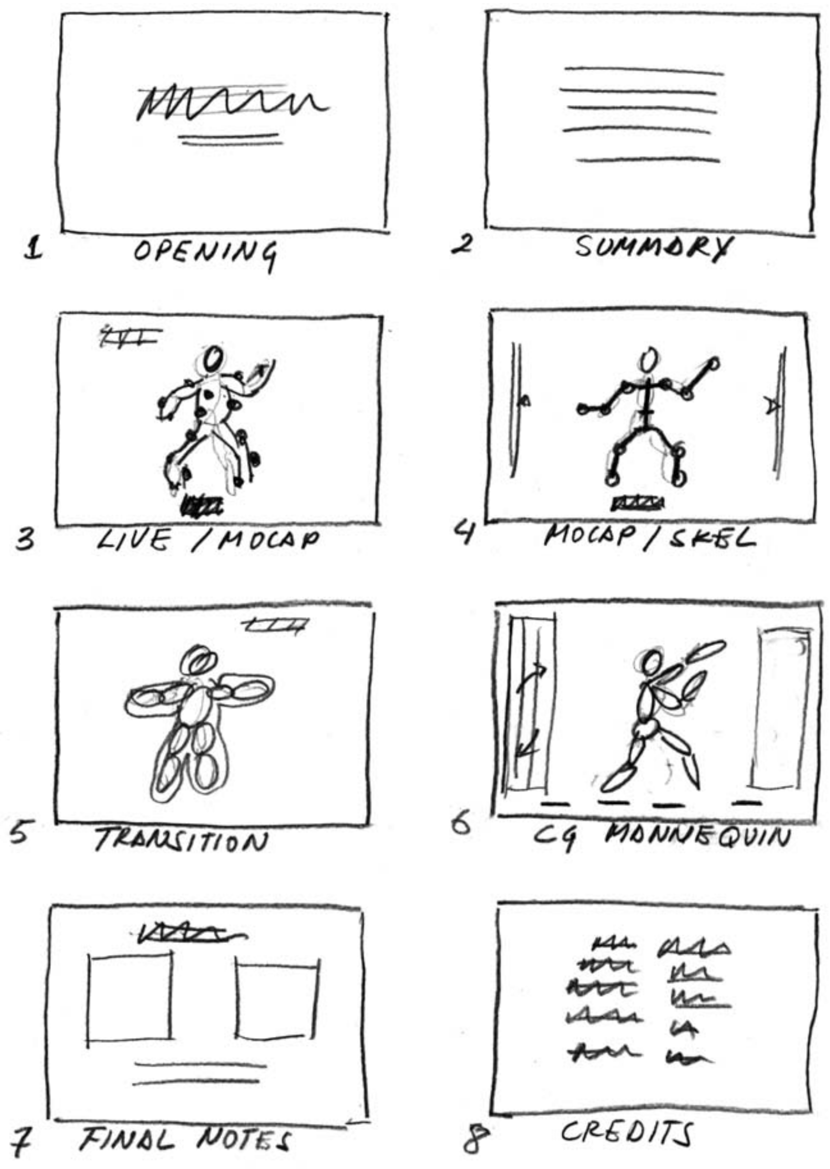

Figure 1.1: Storyboard.

1.2 The Techniques

To produce the video Dance to The Music / Play to the Motion we employed a plethora of techniques that are commonly used in Digital Special Effects and Computer Animated Films.

These techniques span a wide variety of domains, ranging from live action shooting to CG character animation on the visual side, and from music scoring to soundtrack creation on the audio side.

Pipeline

The complete video is generated by series of steps that combine in non-trivial ways the various techniques mentioned above. These tasks form a pipeline of video production, that begins with the argument, storyboard and pre-production planning, continues with shooting and production, and ends with editing and post-production.

In the subsequent chapters of this technical report, we will present in detail each of these techiniques and discuss how they are assembled to produce the video Dance to the Music / Play to the Motion.

More specifically, we wil address the following topics:

- Cinematography
- Motion Capture
- Animation
- Modeling of 3D Characters
- Rendering and Illumination
- Camera Calibration
- Music and Soundtrack
- Motion Graphics
- Editing

Chapter 2

Cinematography

In thsi section we discuss the technical aspects of the live action cinematography.

2.1 Video Format

From the very beginning we decided to make the video in the most advanced standards. This implied that we would use the format *Full HD*, which has an image resolution of 1920×1080 pixels and a frame rate of 60 fps. This choice also determined the wide aspect ratio, 16 : 9, for the image.

Since the first part of the video shows the real dance performance, we had to shoot live action in a studio where the motion capture took place.

Figure 2.1 shows the set for the dance performance. It is actually the main background for the video, because we opted to use a fixed camera a wide shot of the action.

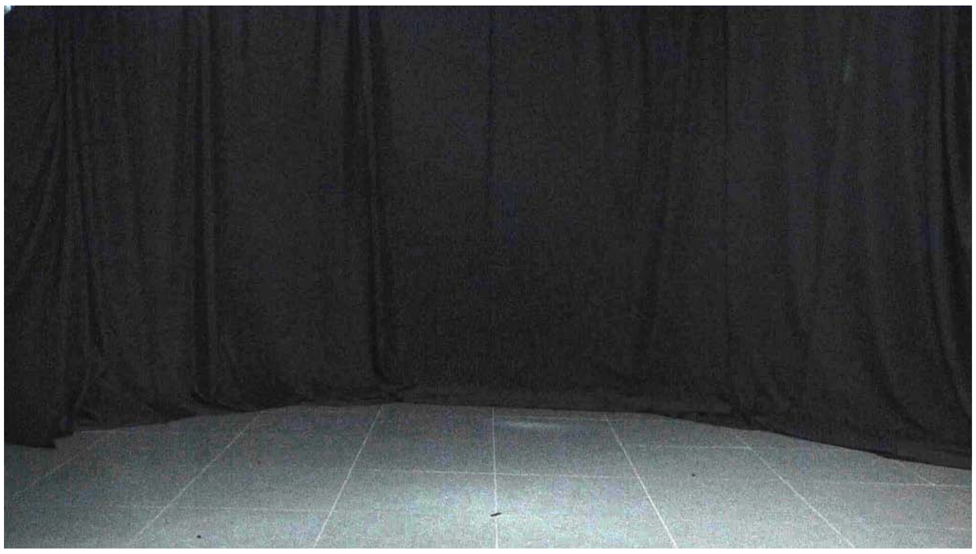

Figure 2.1: Background of HD Frame

The set, as can also be seen in Figure 2.1 was a studio with a dance floor and a dark background. The dancer was wearing a black suit with retroreflective markers.

2.2 Lighting

The lighting was designed to emphasize the motion of the dancer. It consisted mainly of a backlight provided by two 600W Omni reflectors just outside the upper sides of the image frame, as shown in Figure 2.2.

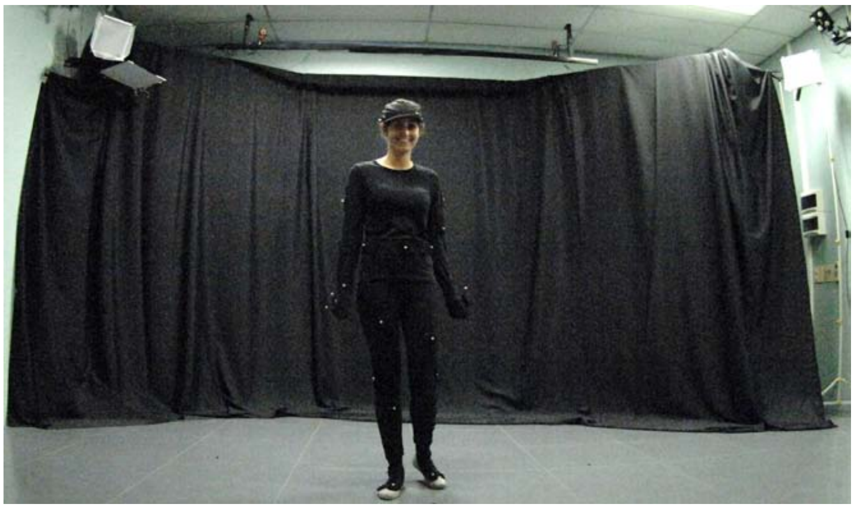

Figure 2.2: Base Illumination: Backlight

The purpose of this base illumination was to mark the silhouette of the dancer without revealing too much of her figure.

The backlight was complemented by a frontal fill light, which consisted of a 200W reflector placed next to the main camera, as can be seen in Figure 2.3. The intensity of this source was carefully balanced to brighten the retro-reflective marker in the dancer's suit, while preserving a high contrast for the backlight effect from the base illumination.

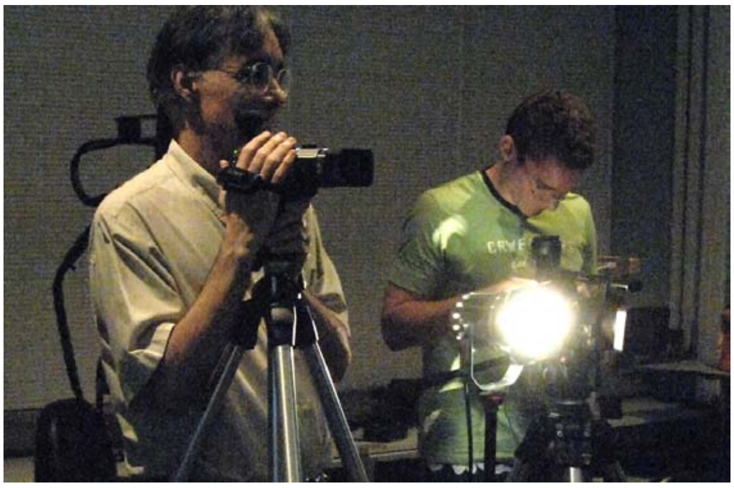

Figure 2.3: Fill Light

2.3 Cameras

The live action part of the video was shot with two cameras: a frontal main camera for wide view coverage of the dance performance and a secondary side camera for close-ups of the dancer. Figure 2.4 shows both cameras positioned at their location in the studio.

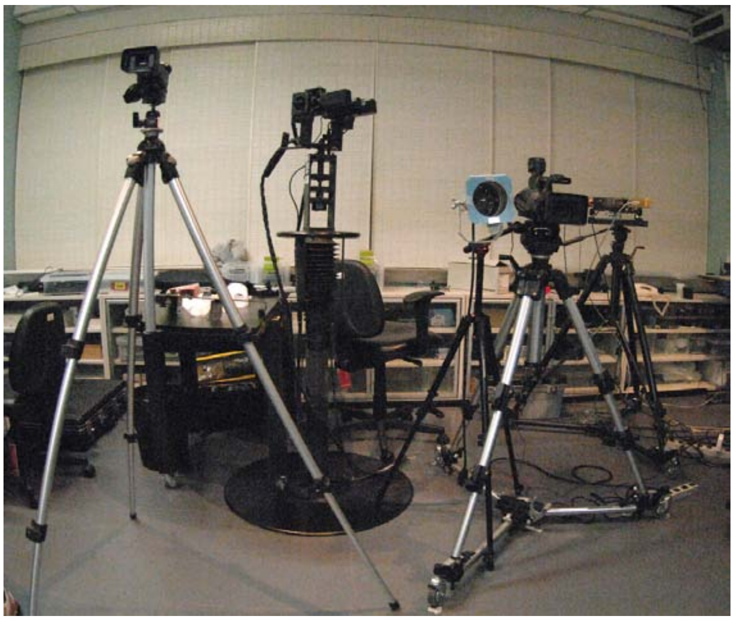

Figure 2.4: Cameras

The main camera was a 3-CCD Panasonic AVCHD video camera, while the second camera was a 1-CCD Sony HDV camera. We used Manfrotto tripods for both cameras. Figure 2.5 shows the capture setup during shooting.

Figure 2.5: Shooting a Scene.

Chapter 3

Motion Capture

Motion Capture (MoCap) is a technology that allows us to record human motion with sensors and to digitally map the motion to computer-generated creatures[1].

The applications of motion capture go far beyond animation and include biomedical analysis, surveillance, sports performance analysis and input mechanism for human-computer interaction. Each application has its own particular set of singularities and challenges.

In this chapter, we will discuss motion capture of full body motion for character animation. We will introduce the basic concepts, detail the technique and describe how it was implemented at the VISGRAF Laboratory.

3.1 Introduction

By definition, to animate is to bring to life, in this case, to make a lifeless object (a graphics model) move. Realistic animation of human motion is a challenging task, firstly, because human movements can be quite complex since joints have many degrees of freedom and, secondly, because people are skilled at perceiving the subtle details of human motion. For example, people are capable of recognizing friends at a distance purely from the way they walk and can perceive personality and mood from body language. This implies that synthetic human motion needs to be very accurate in order to appear real.

It is the opinion of many researchers of the area that synthesis of realistic human motion can only be made possible by an approach that makes extensive use of data from the real world [2]. It this context, it has been quite appealing for animators to used methods of copying the movements of real life objects.

An early example of such a technique is Rotoscoping, in which animators trace over live-action film movement, frame by frame, in order to create realistic motion. Though archives show that most of Snow White's movements were traced from actors motions using this technique, Wald Disney never admired to it. In fact, this was consider "cheating" because it was not produced by the imagination of the artist and also "cheep animation" because animations were supposed to be "bigger than life" not merely a "copy of life" [1].

Rotoscoping was, naturally, a precursor of MoCap and the controversy around it has the same origin. On the one hand, there is the need for creating engaging and expressive characters and on the other hand the need of synthesizing realistic motion efficiently and fast. Therefore, withing the animation community, there is a historical tension between animators and MoCap technicians [3].

The techniques for motion creation are usually divided into three basic categories: manual specification (key framing), motion capture and simulation [4].

Key framing borrows its name from traditional hand animation and is, in fact, very similar to it in the sense that, while computers reduce some of the labor by automatically interpolating between frames, the animator has to specify critical (or key) positions for the objects. This requires great training and talent, since a characters usually have many controls (e.g, each of the main characters of the movie Toy Story, which were animated in this fashion, had more than 700 controls). The advantage of this method is that the artist is able to control subtle details of the motion. Nevertheless, it is very hard to make the characters look real.

Motion Capture, as we have mentioned above, is a process that transfers recorded movement to an animated object. Some of the advantages of motion capture over traditional computer animation are [5]:

- more rapid, even real time results;
- real, naturalistic movement data;
- extremely accurate 3-D data that permits the study of the essence of the movements; and
- data formats that require minimal storage and allow for easy manipulation and processing.

The physically based approach, uses laws of physics to generate motion through simulation and optimization. This technique is largely used, not only for human motion, but also to animate fluids, fire, explosions, face and hair. Simulation techniques supply physical realism, while MoCap allows for natural looking motion. Currently, many applications merge both techniques together in order to create models of human motion that are flexible and realistic [2].

3.2 MoCap Technique

Motion Capture systems can be divided into three different categories [5]: inside-in (sensors and sources located on the body), inside-out (sensors located on the body and sources outside) and outside-in (sources located on the body and sensors outside).

An example of an inside-in system is an electromechanical suit, where sensors are attached to to the performer's body measuring the actual joints inside the body. The advantages of this method are the absence of occlusions (all sensors are always "visible") and the portability of the suits. Nevertheless the actor's movement are constrained by the armature.

In electromagnetic (inside-out) systems, electromagnetic sensors, placed on joints of the moving object, measure their orientation and position with respect to an electromagnetic field generated by a transmitter. This method also directly collects positions and orientations of the sensors and does not have to consider occlusion problems. The drawbacks of this technique relate to the range and accuracy of the magnetic field as well as the constraint of movement by cables.

Optical systems are inside-out systems which use data captured from image sensors to triangulate the 3D position of a subject between one or more calibrated cameras. Data acquisition is traditionally implemented using special retro-reflexive markers attached to an actor and infrared cameras. However, more recent systems are able to generate accurate data by tracking surface features identified dynamically for each particular subject. This is called the marker-less approach.

Optical techniques are widely used since they allow large performance areas (depending on the number of cameras) and performers are not seriously constrained by markers. Nevertheless, orientation information is not directly generated and therefore extensive post-processing needs to be done in order to reconstruct the three dimensional motion.

The three major tasks that need to be undertaken are [6]: markers have to be identified and correlated in the 2D images, 3D locations have to be constructed from the 2D locations, and 3D marker locations need to be constrained to the model being capture (e.g., human skeleton).

The first step is to find the markers at each frame and track them over the video sequence. The latter can be quite difficult because markers often overlap, change position relative to one another and are occluded. In addition, noise can arise from the physical system (markers may move relative to their initial positions) or the sampling process. Hence three major problems occur when tracking the markers and may need user interventions to be resolved: missing data in the presence of occlusions, swapped paths between two markers that pass within a small distance of each other, and noise.

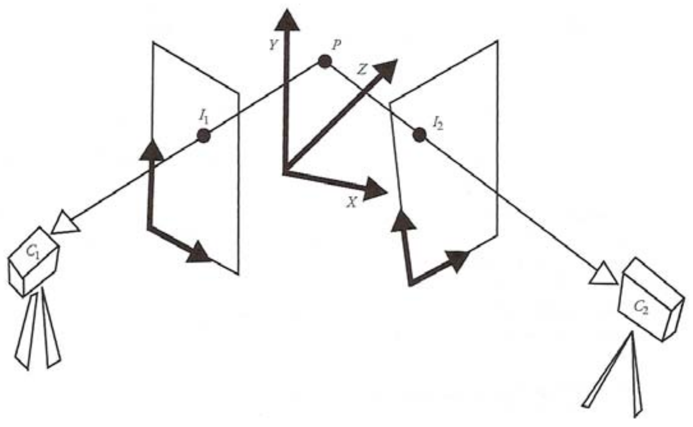

Figure 3.1: Two-camera view of a point. Extracted from [6].

The second step is to reconstruct the 3D points from the 2D trajectories. For this purpose, cameras need to calibrated , i.e., the position, orientation and intrinsic properties of the cameras need to be known. This can be done by recording a number of image points whose locations are known. With calibrated cameras, the three dimensional coordinates of each marker can be recontructed from at least two different views (the more orthogonal the views the better), as shown in Figure 3.1.

Finally, the 3D marker positions need to be transformed into the motion parameters of a kinematic skeleton model. For this, it is crucial to place the markers in adequate positions. The markers cannot be located exactly on the joint firstly because they are placed on the surface of the skin and second because they have to be set in positions where they will not move according to the performance. This represents a problem because although distances between consecutive joints are always the same, distances between markers may vary. Therefore, in order to locate the joint relative to the marker, we need not only the position, but also the orientation.

To solve these problems, most standard formats require placing three non-linear markers on each rigid body part instead of one in each joint [7]. These locations are then used to determine the position and orientation of each limb and the skeleton configuration is determined while the tracked subject performs an initialization pose (T-pose). Since noise is usually added to the data, directly using the calculated joint positions will probably result in varying bone lengths. To get around this problem, many systems calculate joint rotations and use a skeletal hierarchy to reconstruct the pose of the articulated body.

3.3 MoCap at Visgraph

There are currently several comercial MoCap System available. During the course of this project, motion capture was done in the VISGRAPH Laboratory using OPTITRACK, `NaturalPoint`'s optical MoCap System. The infrared cameras (see Figure 3.2.b) are sensitive to the retroreflexive markers (see Figure 3.2.b) which are placed in the performer's body.

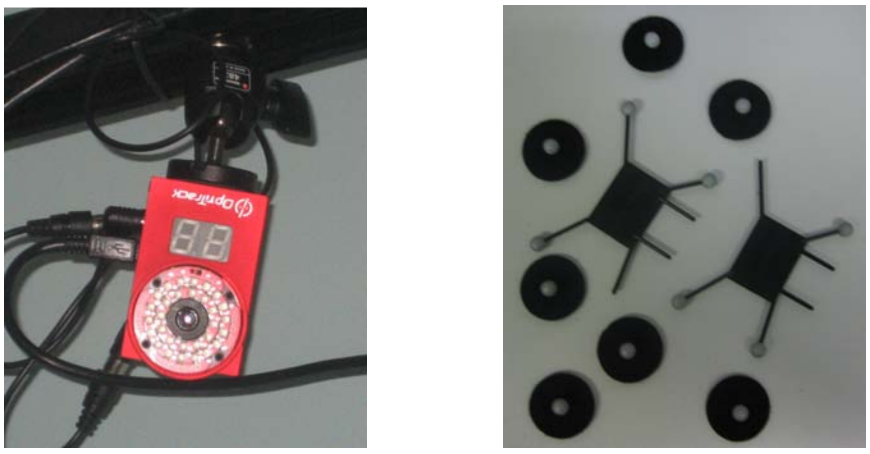
(a) OPTITRACK camera (b) Retroreflexive markers

Figure 3.2: MoCap setup.

As with traditional animation and many other arts, MoCap is actually composed of a number of phases[8]:

- studio set-up,
- calibration of capture area,
- performance and capture of movement,
- clean-up of data, and

- post-processing of data.

The studio was set up with six cameras, as shown in Figure 3.3. Tracking a large number of performers or expanding the capture area is accomplished by the addition of more cameras. Since each marker must be"seen" by at least two cameras, a greater number of cameras diminishes the possibility of occlusions.

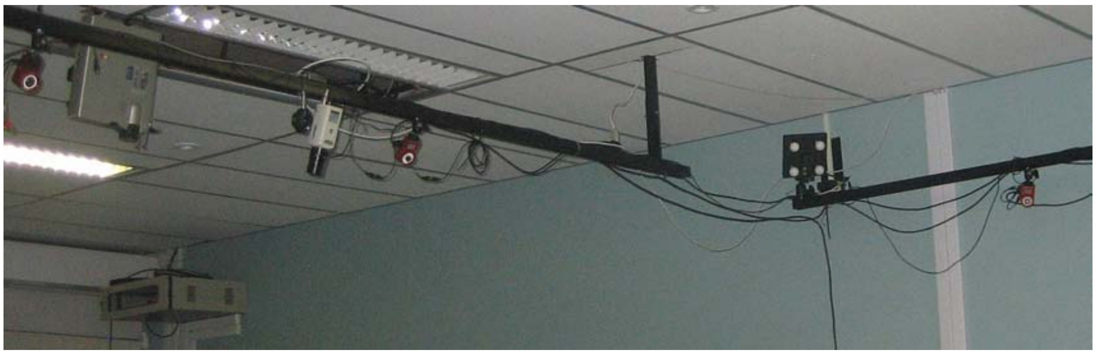

Figure 3.3: OPTITRACK cameras set up at the Visgraf Laboratory.

Camera calibration was done with the help of OPTITRACK's software, AREA. This software also specifies the postion of the markers in the performer's body (see Figure 3.4).

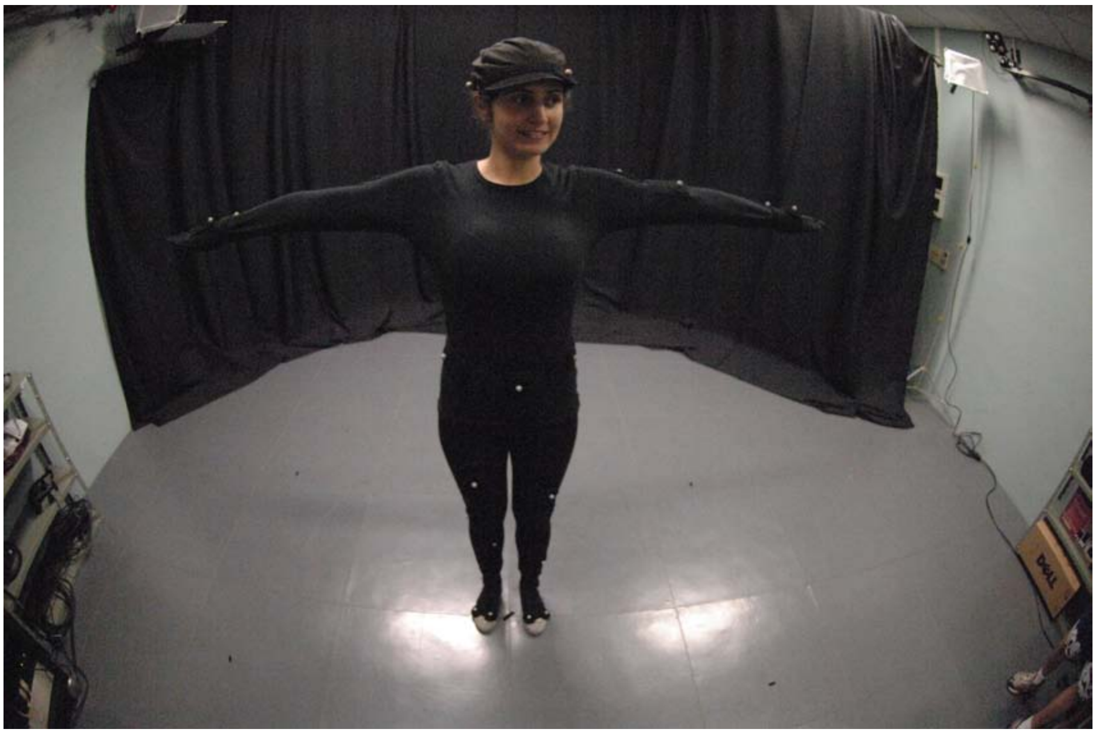

Figure 3.4: Dancer performing at the VISGRAPH Laboratory

The ARENA software (see Figure 3.5) was also used to process the acquired data. The first processing step is to trajectorize the data. This procedure takes the 2D data from each individual camera and changes it to a fully 3D path of each individual marker.

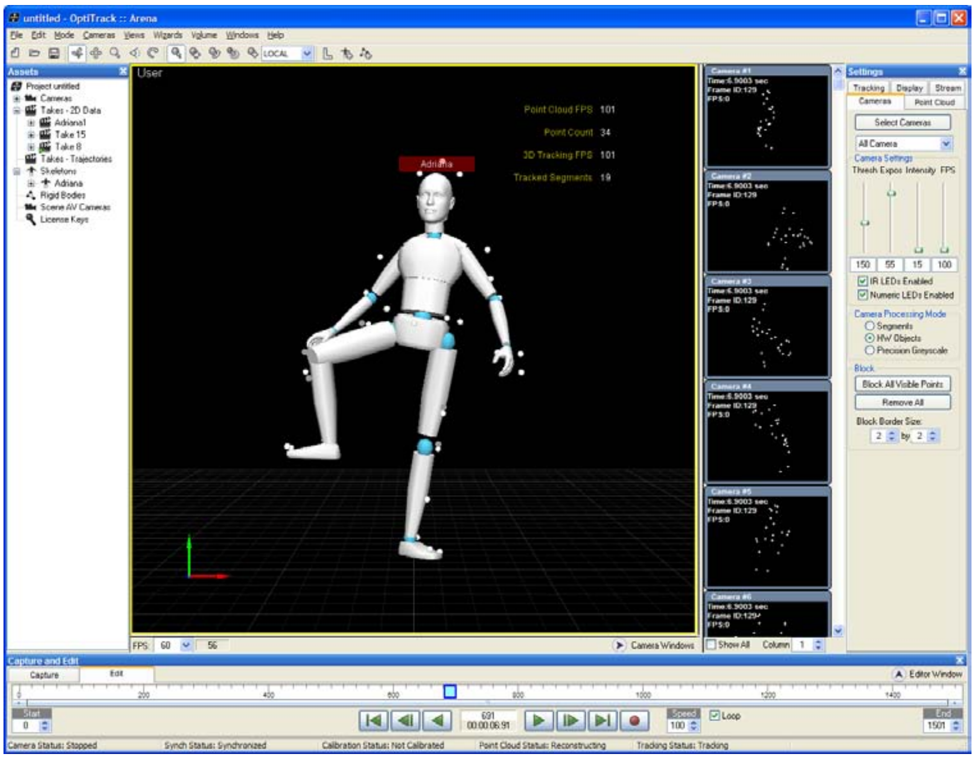

Point Cloud FPS 101
Point Count 34
3D Tracking FPS 101
Tracked Segments 19

Thresh 150, Expos 55, Intensity 15, FPS 100
[✓] IR LEDs Enabled
[✓] Numeric LEDs Enabled
Camera Processing Mode: HW Objects
Block Border Size: 2 by 2

FPS: 60 56

Start 0, 691 00:00:06:91, Speed 100, [✓] Loop, End 1501

Camera Status: Stopped Synch Status: Synchronized Calibration Status: Not Calibrated Point Cloud Status: Reconstructing Tracking Status: Tracking

Figure 3.5: The ARENA software.

After this procedure the software allows for post capture editing (such as filling gaps, fixing swaps and smoothing tracks) and exporting a file in a BVH or C3D format.

In this project, we used the BVH file format, which was originally developed by Biovision, a motion capture services company, as a way to provide motion capture data to their customers. Nowadays, it is widely used, and many applications support importing and exporting files in this format. It consists of two parts, a header section which describes the hierarchy and initial pose of the skeleton, and a data section which contains the motion data. For a more detailed description of the BVH file format, see Appendix A.

Chapter 4

Animation

4.1 Introduction

In the previous chapter we discussed Motion Capture and its applications to character animation. Though the technique is very powerful in the sense that it allows rendering natural and realistic motion, MoCap by itself is nothing more than a method for reproducing acquired movements. Therefore, much effort has been, and is currently being, put into extending the applications of MoCap data.

There are many reasons that make editing captured motion extremely important. Firstly, it is usually necessary to eliminate artifacts generated during acquisition. Secondly, it is important to match time and space of computer generated environments, overcome spatial constraints of capture studios and allow for the existence of motions that would be extremely hard for an actor to perform, such as the ones used in special effects. Finally, it is interesting to be able to reuse motion data in different occasions. For example, given a walking scene, it should be possible to generate a walk on an uneven terrain or steeping over an obstacle.

In addition to editing [9, 10], it is the interest of many researches in the field to synthesize new streams of motion from previously acquired data and, therefore, be able to create new and more complex motions. Motion synthesis strategies include constructing models of human motion [11, 12], interpolating motion to create new sequences [13] and reordering motion clips employing a motion graph [14].

In this work, we use a motion graph to create a new motion stream from previously acquired data. We introduced a couple of restricted to this graph, so it could used as a tool to guide the concatenation of musical phrases for the composition of a new song.

In the next section we describe how a motion graph is built and in section 4.3 we discuss the *choreo.graph*, a measure-synchronous motion graph which was implement for the purpose of this project.

4.2 Motion Graphs

Motion graphs were introduced in [14], in order to encapsulate connections among a database. In this graph, edges correspond to motion clips (sequence of frames) and nodes to choice points (specific frames) connecting these clips. After selecting the similar frames, or windows of frames, and creating the graph connections, a walk along the graph allows us to re-assemble the captured clips, creating new motion.

Figure 4.1 illustrates the construction of a motion graph. Initially we have two clips of motion from a MoCap database. The resulting graph is the one shown in Figure 4.1(a), which is disconnected and quite simple. Notice that it is possible to add nodes in the graph, simply by breaking the initial motion clips into two or more small clips, as shown in Figure 4.1(b). Nevertheless, this graph is still disconnected.

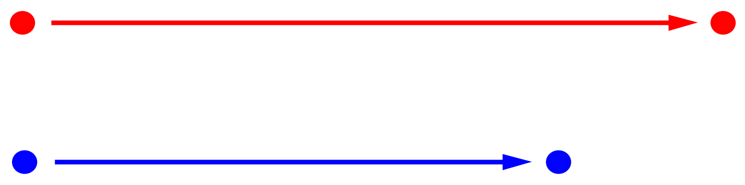
(a) Initial graph.

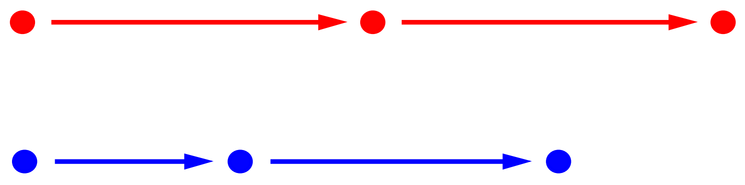
(b) Adding new nodes.

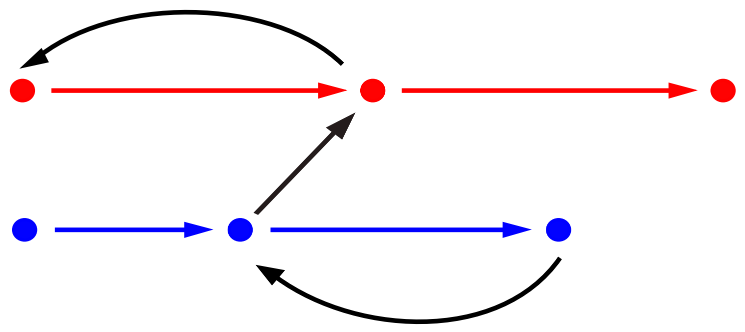
(c) Create greater connectivity.

Figure 4.1: Construction of a motion graph.

To create greater connectivity, we introduce transition clips, as shown in Figure 4.1(c). Notice that these new edges also represent clips of motion which have to be synthesized by the technique. Therefore in order to create these new edges we first have to select the nodes which can be efficiently connected and then create the motion clips to which the transition edges will correspond.

Following the ideas proposed in [14], we select the nodes which are sufficiently similar so that straightforward blending is almost certain to provide valid transitions and use a similarity norm that takes into account a sequence of frames and a point cloud driven by the skeleton.

As in the BVH file, a motion frame is fully described by the position and orientation of the root node and the rotation of the other joints. However, an attempt to use this information to calculate similarity between frames will be highly unsuccessful because some of these parameters have a much greater overall effect on the characters position than others (for example, a knee rotation is usually much more significant than a wrist rotation). In addition, it is quite hard to set fixed weights that work well in all cases, since the effect of a joint rotation on the shape of the body depends on the current configuration of the body.

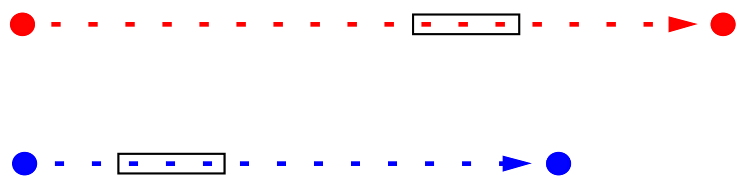
(a) Similar sequence of frames.

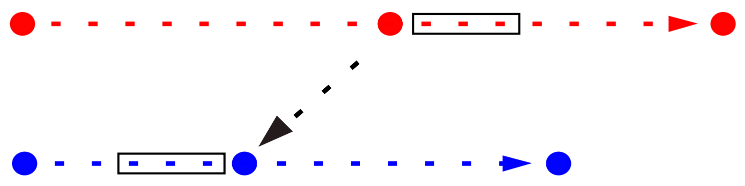
(b) Added connection.

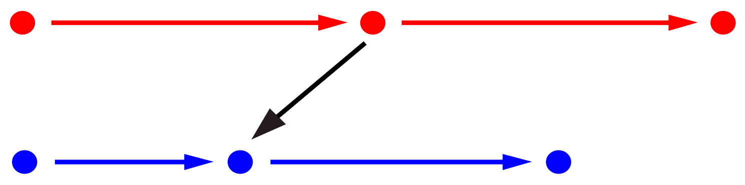
(c) Resulting graph.

Figure 4.2: Addition of a transition edge.

To solve this problem, we use a point cloud, which describe the skeleton pose (ideally this point cloud is a downsampling of the mesh defining the character) and vector distance norm. It is important to notice that a motion is fundamentally unchanged if we translate it along the floor plane or rotate it about the vertical axis. Therefore, before comparing the distance between two point clouds we apply a rigid 2D transform to the second point cloud that sets it at the optimal position so that weighted sum of squared distances is minimal.

In addition, it is important to consider not only the current position but also derivative information, such as velocity and acceleration. We incorporate this information to the similarity metric by using a window of frames. This also helps the blending procedure. An example is shown in Figure 4.2. The similarity metric selects the two sequences of frames as shown in Figure 4.2(a). Therefore we can add an edge that connects the beginning of first sequence of frames to the end of the second one, shown in Figure 4.2(b). The resulting motion associated to this transition edge is created by blending the two sequences of frames.

Finally, after the edges are created, we prune the graph by computing the strongly connected components (SCCs). We use only the largest SCC so as to guarantee that there are no dead ends, and therefore we can synthesize the motion indefinitely.

4.3 The *choreo.graph*

Songs are metrically organized in measures, which determine the size of the melodic phrases. Therefore, in order to preserve the size of the melodic phrases during composition, it is important to build a *measure-synchronous* motion graph.

Since the performer is dancing according to a song we are able to relate melodic phases to parts of the acquired motion (choreography phrase). Once both informations are synchronized, we can use music metric information to segment the dancer's movement.

A measure-synchronous motion graph is then built by observing segment boundaries similarities. We used the similarity metric described in the previous section, but instead of connecting the nodes which are sufficiently similar, we connect the end of each motion phrase to the five nearest segments, creating a directional *weighted* graph.

A restricted random walk on this graph creates a new motion. We observed that two restrictions are appropriate for the resulting music to resemble samba style pieces. First, musical instruments should not vary too frequently. In our implementation, this is guaranteed by dynamically varying the weights of the graph edges during the walk. Second, it is important to observe intensity variations between large music blocks during composition. We used three distinct blocks, and motion phrases were annotated accordingly. During motion synthesis, the user can specify the number of phrases desired for each block and the order in which they occur.

The *choreo.graph* is not restrict the to the strongly connected components. Instead, the large number of connections in the graph is combined with a weighting system to prevent the walk from reaching the last phrase of each clip, which would be a dead end.

Nevertheless, it would be interesting to reach the end of the clip, since usually dancers perform a "finishing pose". To this end, we use a restricted graph search that allows quickly reaching the last phrase after the total number of phrases (specified by the user) has been concatenated.

The user interface was developed in C++ using QT toolkit. We also implemented a BVH file parser and a player that allows us to compare captured to rendered motion. As shown in Figure 6.3, the interface shows where each part of the rendered motion comes from. The graph transitions (blended motions) are represented in black and the original motion clips in an increasing saturation scale of color.

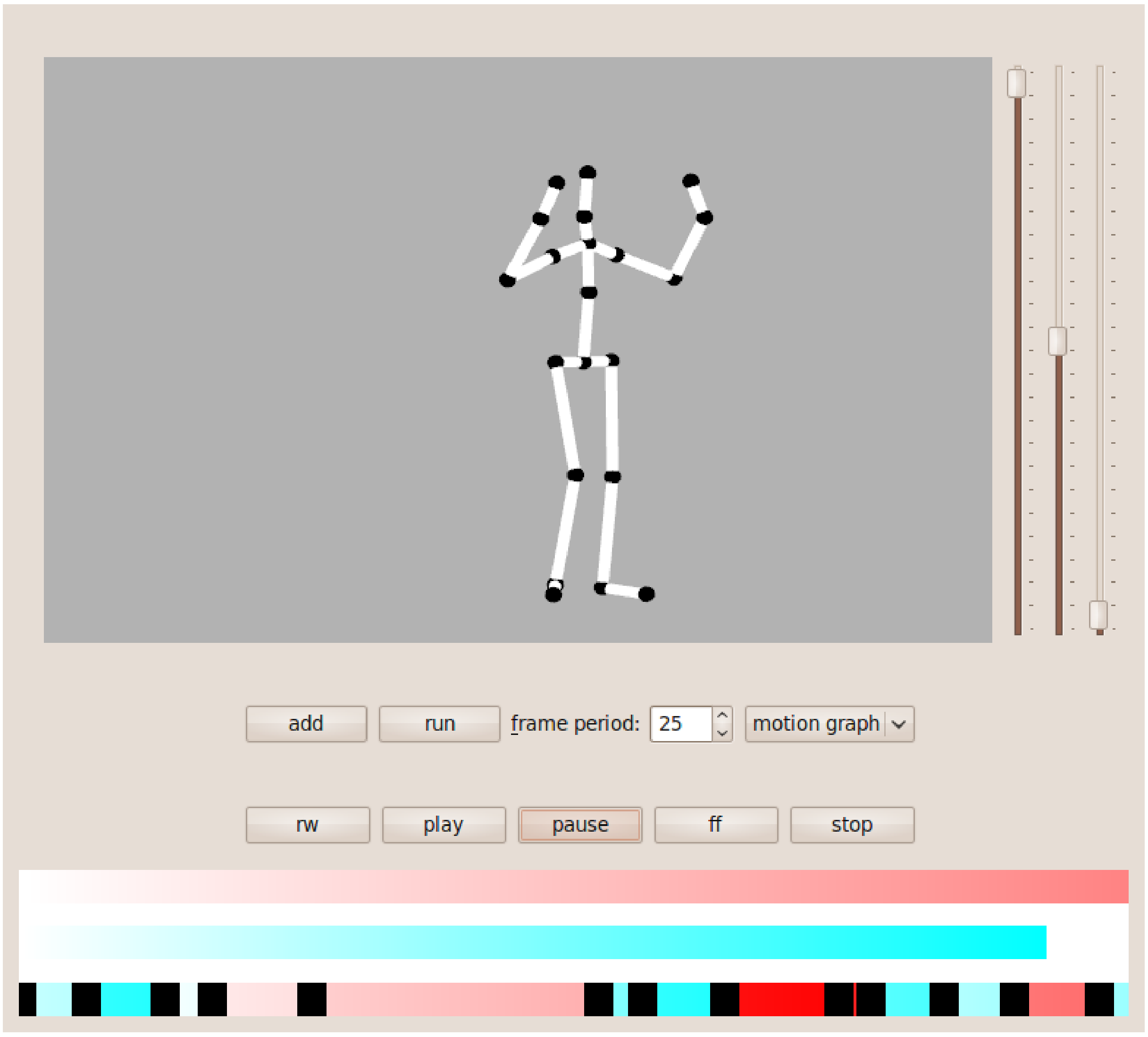

Figure 4.3: User interface that was implemented.

Chapter 5

Modeling 3D Characters

The animation produced as explained in the last chapter was transfered to a mannequin and to a skeleton made of spheres and cylinders. This chapter explains how we did this using Maya.

5.1 Introduction

We can split 3D Characters into two groups, which one demanding a different modeling process:

Articulated Characters They are characters made of rigid bodies connected by joints. The modeling process can be done by parenting nodes that represents these bodies to theirs respective joints in a hierarchy. They are usually used to represent mechanical objects.

Soft characters They consists on deformable surfaces attached to skeletons. The surfaces deforms depending on the skeletons configuration. In the modeling process the user has to specify the influence of each joint over each point of the surface, it is usually done by using painting interfaces. They are usually used to represent organic characters.

On this project we only made use of articulated characters.

There are many good references about modeling characters in Maya. A good introduction can be found in [15], and more detailed explanations are given by [16] and [17].

5.2 Building the character

The first step was importing the BVH animation. It was done by using the MEL script bvhimport.mel written by Sergiy Migdalskiy and available in the site Highend3d.com. After doing it, a skeleton appeared allowing us to check the animation by moving the time line (see Figure 5.1).

It would be possible to map the animation of this skeleton to a 3D model previously modeled. It could be done by using the Character Mapper Tool combined to the Trax Editor. But, we adopted a different solution, we modeled the character directly over this skeleton.

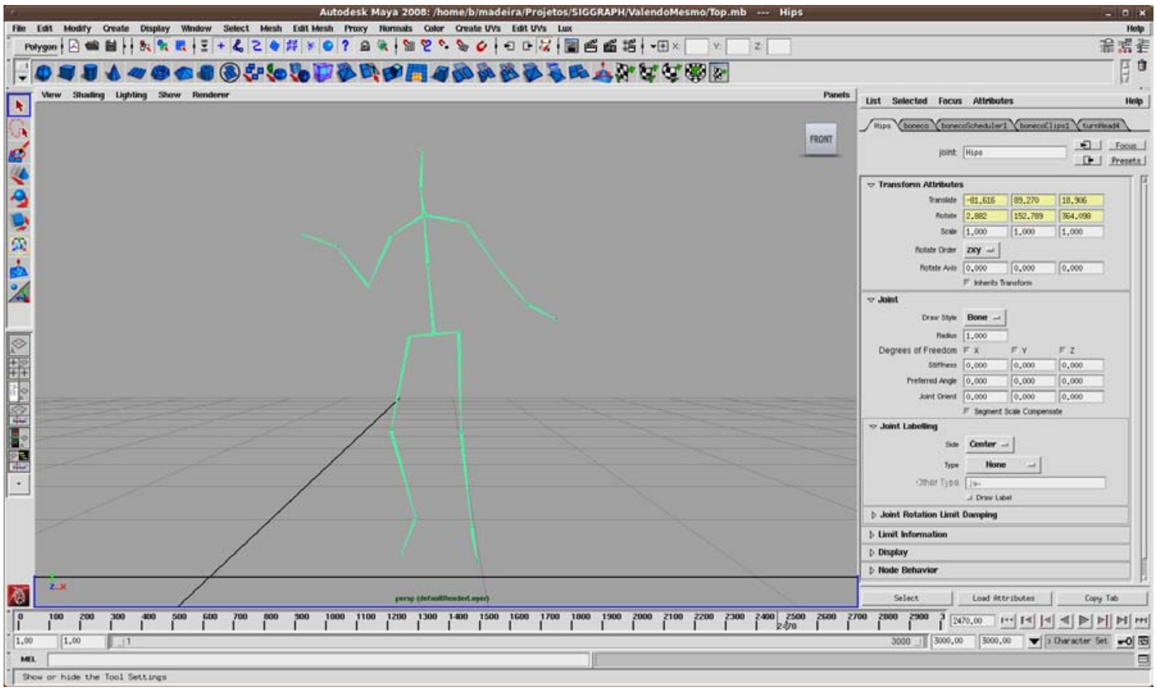
Autodesk Maya 2008: /home/b/madeira/Projetos/SIGGRAPH/ValendoMesmo/Top.mb --- Hips
File Edit Modify Create Display Window Select Mesh Edit Mesh Proxy Normals Color Create UVs Edit UVs Lux
View Shading Lighting Show Renderer Panels
FRONT
List Selected Focus Attributes Help
joint: Hips
Transform Attributes
Joint
Joint Labelling
Joint Rotation Limit Damping
Limit Information
Display
Node Behavior
Select Load Attributes Copy Tab

Figure 5.1: The skeleton created after importing the BVH animation.

Accessing the Hypergraph Editor we could see the skeleton hierarchy exported by the Arena software as shown in Figure 5.2.

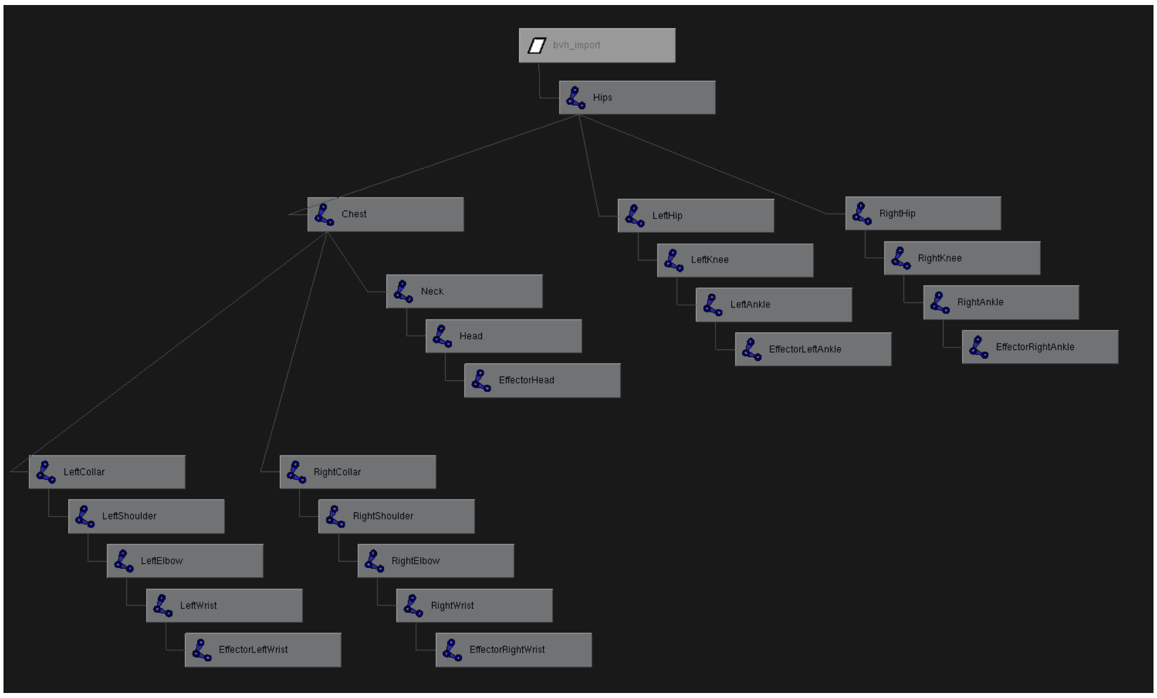

Figure 5.2: The hierarchy of a character exported by Arena.

We moved the skeleton to a T-pose by setting the time line to a negative value. Then, we created the spheres and cylinders and placed them over the bones (see Figure 5.3).

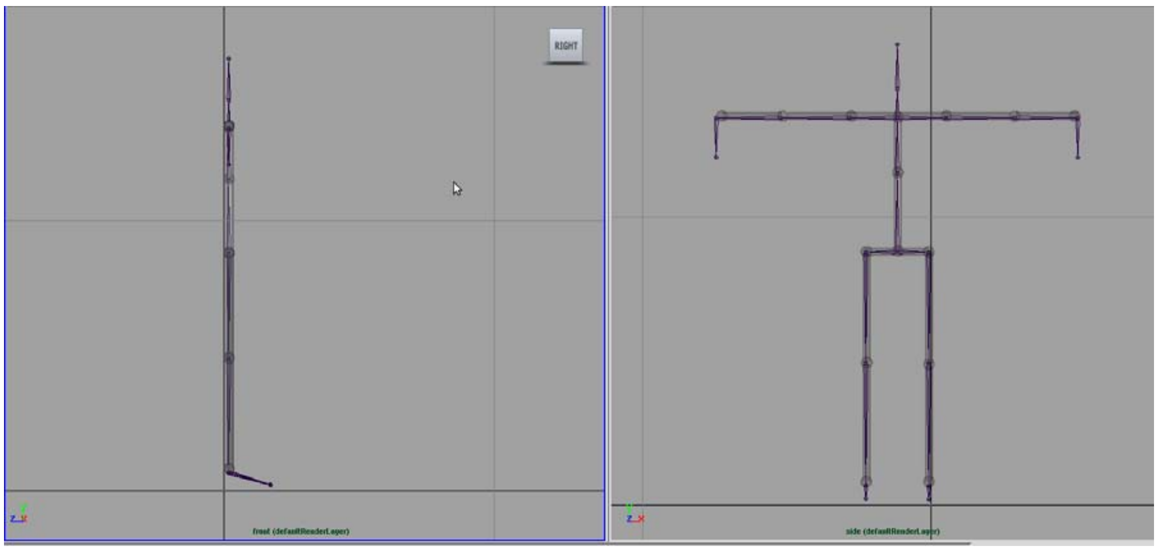

Figure 5.3: The character made of cylinders and spheres.

After displacing the primitives over the bones, we attached them to theirs respective joints using the Hypergraph Editor. The result after parenting all primitives is shown in Figure 5.4.

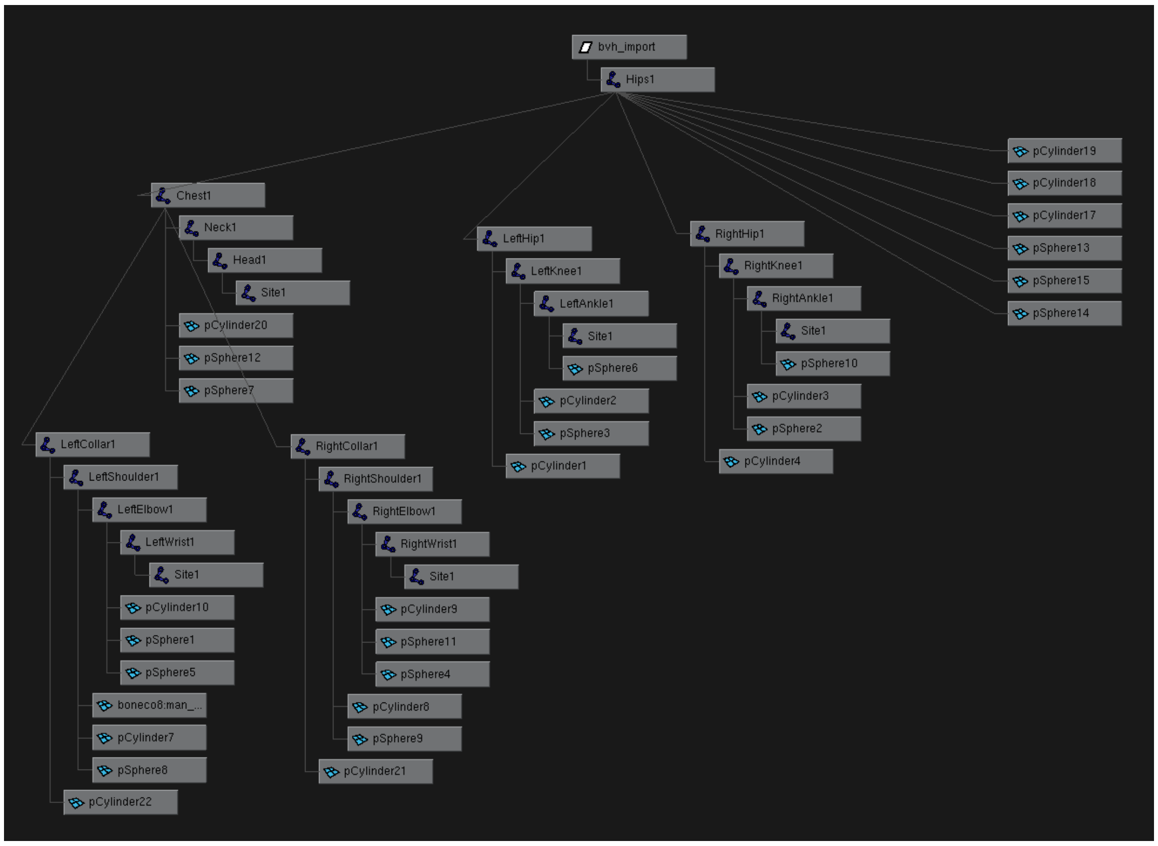

Figure 5.4: The hierarchy of the character made of cylinders and spheres.

The mannequin was created by using a similar process. We made use of the pieces from the mannequin given by the book [18]. The result is presented in the pictures 5.5 and 5.6.

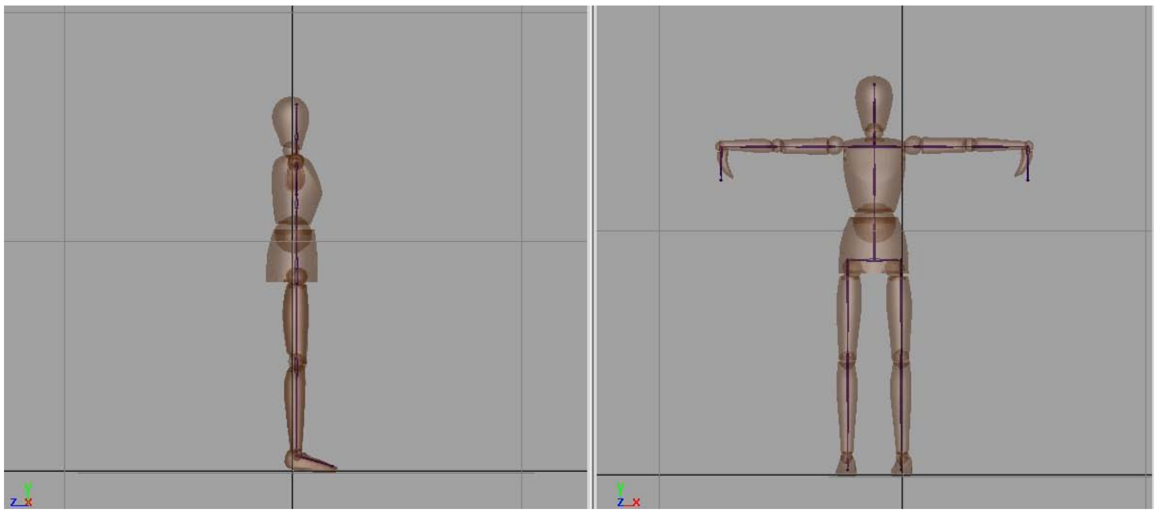

Figure 5.5: The geometry of the mannequin.

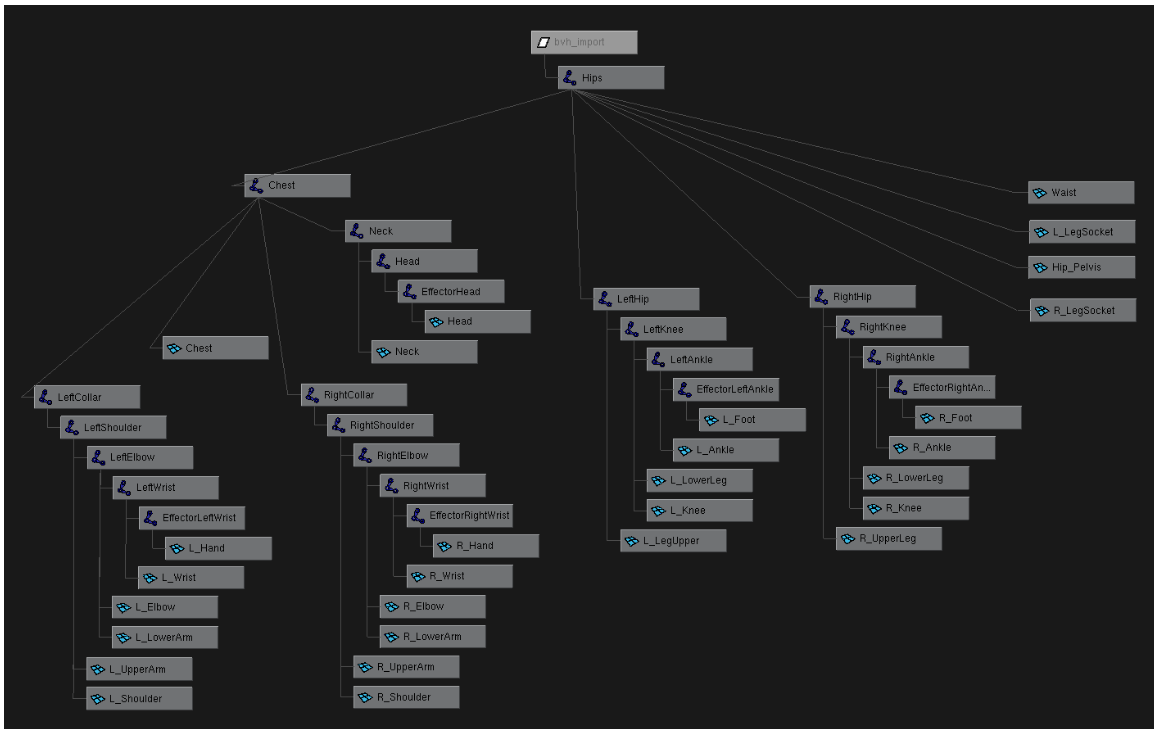

Figure 5.6: The hierarchy of the mannequin.

After modeling the geometry and parenting all primitives, we adjusted the surface material. We chose a Blinn material, where we mapped the wood texture presented in Figure 5.7 to the Color and Bump Mapping attributes.

After adjusting the attributes of the Blinn material we achieved the final look presented in Figure 5.8.

Figure 5.7: The texture used in the mannequin.

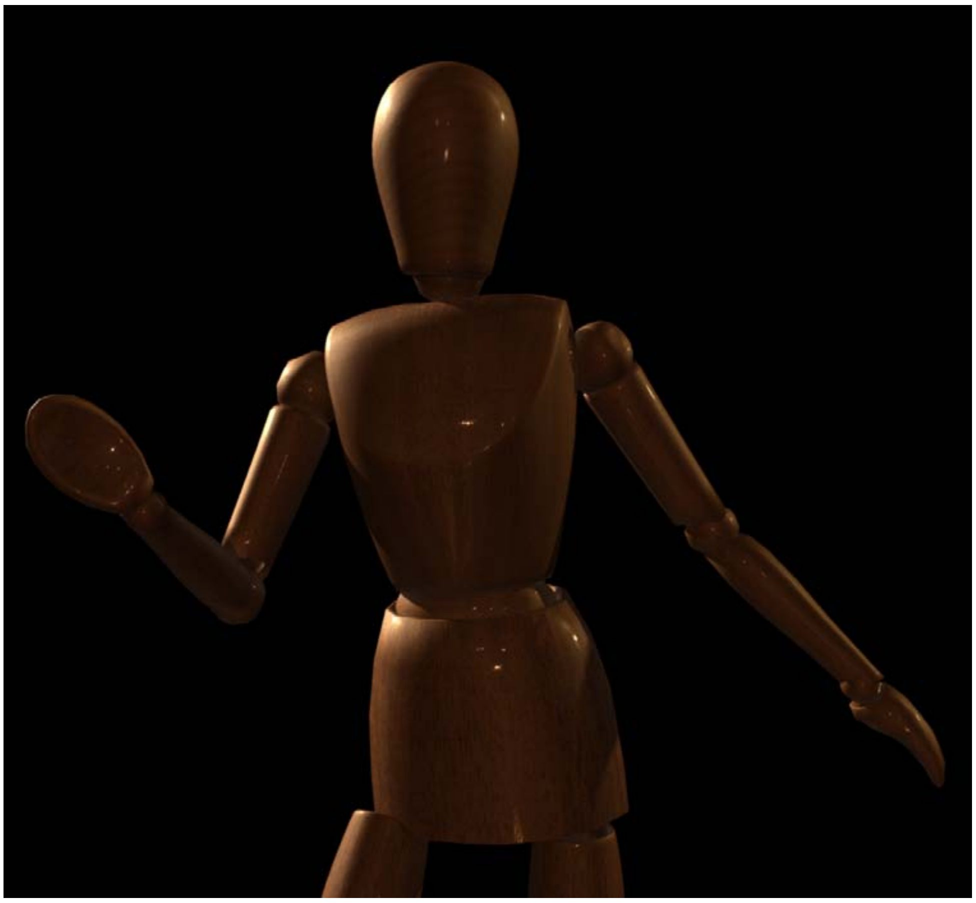
Figure 5.8: The final look of the mannequin.

Chapter 6

Rendering and Lighting

6.1 Introduction

Traditional cameras were set up to record the light so that it could be reproduced on photographic paper, while digital cameras, on the other hand, were developed to reproduce the light captured on a monitor. Neither displays nor photo papers can represent the entire dynamic range of illumination. However, if taken many photos with different exposure times, these images can be combined so that the dynamic range is approximately recovered. With this technique, a series of images can be combined into a single image with high dynamic range (*HDR*), called radiance map.

Because *HDR* images store the full range of light reaching a point in space, they contain information about the shape, color and intensity of direct light sources, as well as the color and distribution of the indirect lighting surfaces from the rest of the scene. Using appropriate rendering algorithms, and sampling techniques, we can efficiently use *HDR* to accurately simulate how objects and environments would be if they were illuminated by light from the real world. This process of using images as light sources is called *image-based lighting* (*IBL*), and was introduced by Paul Debevec [19].

The first step in working with lighting by artificial lighting scenes taken from a real environment, is to store the illumination of the real environment. One way of doing this is by obtaining an omnidirectional, high dynamic range image that records the incident illumination conditions at a particular point in space. An image with this features is called of *Light Probe.*

6.2 Making a Light Probe

There are several techniques for mounting a Light Probe. In this paper we choose one of these forms and further proceed to explain the process followed in the construction of the Light Probe.

The selected method

One method for obtaining a Light Probe is to take a high-dynamic range image of a mirrored ball. Assuming an orthogonal camera, then in theory a single photograph of the mirrored ball can see in all directions, such as in figure 6.1. That is, anything visible from the viewpoint of the mirrored ball will be visible to the camera as a reflection in the ball.

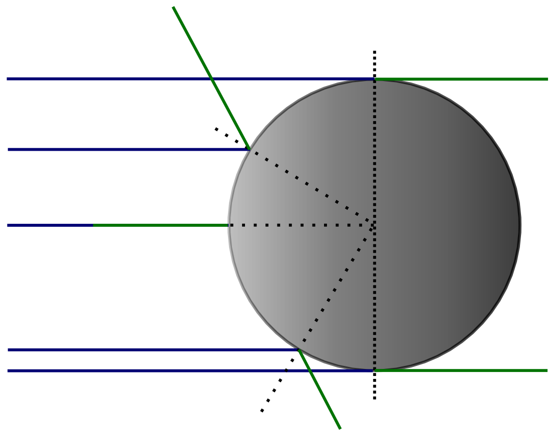

(a)

Figure 6.1: How the rays of the world are reflected into mirrored ball assuming an orthographic camera. The blue rays are the reflections of the green scene rays.

Unfortunately, things that are reflected near the edge of the ball will become extremely stretched and distorted, giving a poor image when it is unwarped. Additionally, in the center of the ball will be a reflection of the camera used to take the photograph, which will obscure some of the background.

To alleviate these problems, we can take two pictures of the mirrored sphere from different angles and blend them together to remove the camera and the regions of poor sampling.

Since the two bad spots in the mirrored ball are directly towards the camera, and directly away from the camera, the two pictures should be taken from positions 90° apart from each other. This way the regions of bad sampling and camera interference will be in different locations in the two images. (Note that taking the images from opposite sides of the ball will not work, as the region of bad sampling in one image will be the location of the camera in the other image, and vice versa.)

In our case we use only one point of view to get the *HDR* image. The camera was placed so that it does not obstruct any light source, the poor sampling region is a black curtain and the map will be used only to illuminate an object that does not contain mirrored reflections. The previous method is recommended in scenes containing several objects with interreflections, where any problem on the map will be seen in these reflections.

Taking LDR Photos and assembling the HDR image

Since we need an *HDR* image of the mirrored ball, we should proceed according to Debevec and Malik [20], building an *HDR* image from a series of *LDR* photos, by reconstructing the response curve. The used camera is not orthogonal, but placing it at a distance about 1.5m and zooming it we can obtain an very small angle of view (fov) approaching an orthogonal projection (figure 6.2). We took care to place the camera in a position that does not obstruct the reflection of none light in mirrored ball and the lights stay in the central area of the ball, where the sampling is better. In the peripheral zone of the ball was a reflection of the black curtain background. Thus it was only enough to take photos with a single camera position.

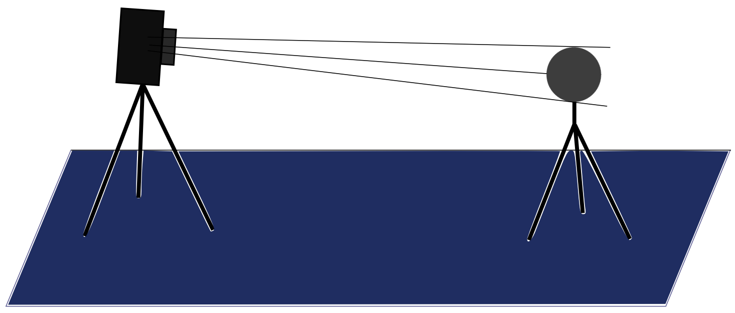

(a)

Figure 6.2: The relative position of the camera an mirrored ball.

First, with the camera fixed on the tripod took several photos of the mirrored ball using a fixed aperture (F8.0) and varying the exposure time (doubling the time between each exhibition from 1/500Sec to 15Sec). We used 14 photographs for construc the map. (figure 6.4(b)).

After the photos were taken, the next step is construct an *HDR* image with them, using *Pfstools* package. Opening the *Qtpfsgui* graphical interface and clicking on "**New Hdr...**" it will open a window where we click it on "**load images**" and select the 14 images of the pictures we took. The program will load the pictures and automatically fill in values for the exhibition EV of each image (figure 6.3(a)). This still can be edited by the user if he deems it necessary. Then we click on "**next**" and move to another screen (figure 6.3(b)) where it is possible to align the images to eliminate possible tripod and camera movements during the series of photographs. Completed the alignment clicking on "**next**" to pass to the next stage.

This is the last window (figure 6.4(a)), where we choose the function of weights, the model of response curve and *HDR* model construction desired. Made the choice we click in "**finish**" and return to the main window where will appear the *HDR* image resulting from the process. Finally keep this file in *.hdr* format to continue editions in other software.

Crop the Mirrored Ball of the result HDR image

The next step is to crop the result *HDR* image to the very edge of the mirrored ball:

First make sure that the "**Circle**" option is checked. This can be found in the Select menu under Draw Options. Checking this will draw an ellipse inscribed in your selection rectangle, which can be useful for matching up the edge of the mirrored ball with your selection.

If the mirrored ball goes off some of the edges in your photograph, make sure that the "**Restrict Selection to Image**" option is unchecked. This can be found in the Select menu under Select Options. Unchecking this will allow the selection tool to select regions outside the bounds of the image.

Select the region around the mirrored ball, and adjust it until the circle borders the edge of the ball (figure 6.5(a)). It should look something like the image below.

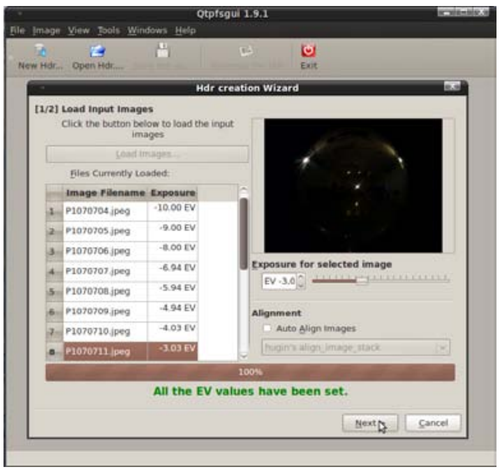
Qtpfsgui 1.9.1
File Image View Tools Windows Help
New Hdr... Open Hdr... Exit
Hdr creation Wizard
Load Images...
Next
Cancel

[1/2] Load Input Images

Click the button below to load the input images

Files Currently Loaded:

	Image Filename	Exposure
1	P1070704.jpeg	-10.00 EV
2	P1070705.jpeg	-9.00 EV
3	P1070706.jpeg	-8.00 EV
4	P1070707.jpeg	-6.94 EV
5	P1070708.jpeg	-5.94 EV
6	P1070709.jpeg	-4.94 EV
7	P1070710.jpeg	-4.03 EV
8	P1070711.jpeg	-3.03 EV

Exposure for selected image: EV -3.0

Alignment

Auto Align Images: hugin's align_image_stack

100%

All the EV values have been set.

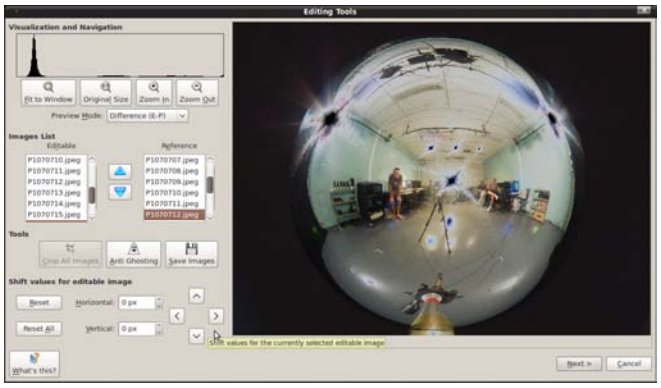

Visualization and Navigation

Preview Mode: Difference (E-P)

Images List

Editable	Reference
P1070710.jpeg	P1070707.jpeg
P1070711.jpeg	P1070708.jpeg
P1070712.jpeg	P1070709.jpeg
P1070713.jpeg	P1070710.jpeg
P1070714.jpeg	P1070711.jpeg
P1070715.jpeg	P1070712.jpeg

Tools

Shift values for editable image

Horizontal: 0 px

Vertical: 0 px

(a) (b)

Figure 6.3: (a) Select the mirror ball with the circle option cheked in the crop tool,(a) The panoramic transformation window, used to transform from the Mirrored Ball format to Latitude/Longitude format.

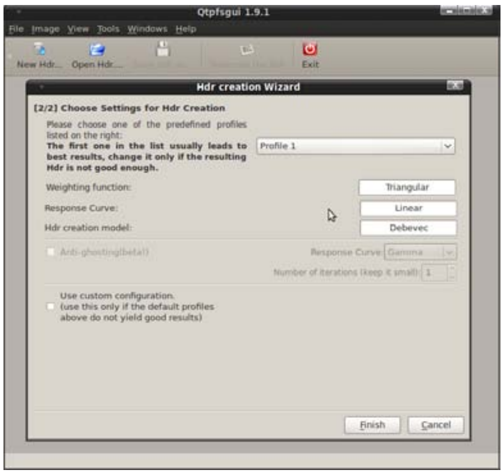
Qtpfsgui 1.9.1
File Image View Tools Windows Help
New Hdr... Open Hdr... Exit
Hdr creation Wizard
Finish
Cancel

[2/2] Choose Settings for Hdr Creation

Please choose one of the predefined profiles listed on the right:
The first one in the list usually leads to best results, change it only if the resulting Hdr is not good enough.

Profile 1

Weighting function: Triangular

Response Curve: Linear

Hdr creation model: Debevec

Anti-ghosting(beta!) Response Curve: Gamma

Number of iterations (keep it small): 1

Use custom configuration. (use this only if the default profiles above do not yield good results)

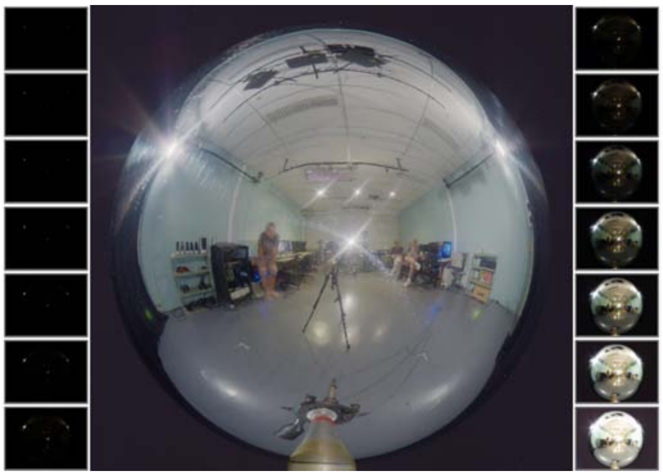

(a) (b)

Figure 6.4: (a) Select the mirror ball with the circle option cheked in the crop tool,(b)The *HDR* image of mirrored ball assembled with the 14 *LDR* photos of the left and right side.

When you have the circle lined up, crop the image using the Crop command in the Image menu.

Apply the mirrored to latitude-longitude transform

Finally, when we have the crop of the mirrored ball, we transfomer it to latitude-longitude format. We chose the menu "**Image**"→"**Panorama**"→"**Panoramic Transformations**"will open a window like the figure 6.5(b) where we put the desired transformation, of "**Mirrored Ball**"to "**Latitude/Longitude**"and clicking on "**ok**". Thus we get a new image in the desired format (Figure 6.6(b)).

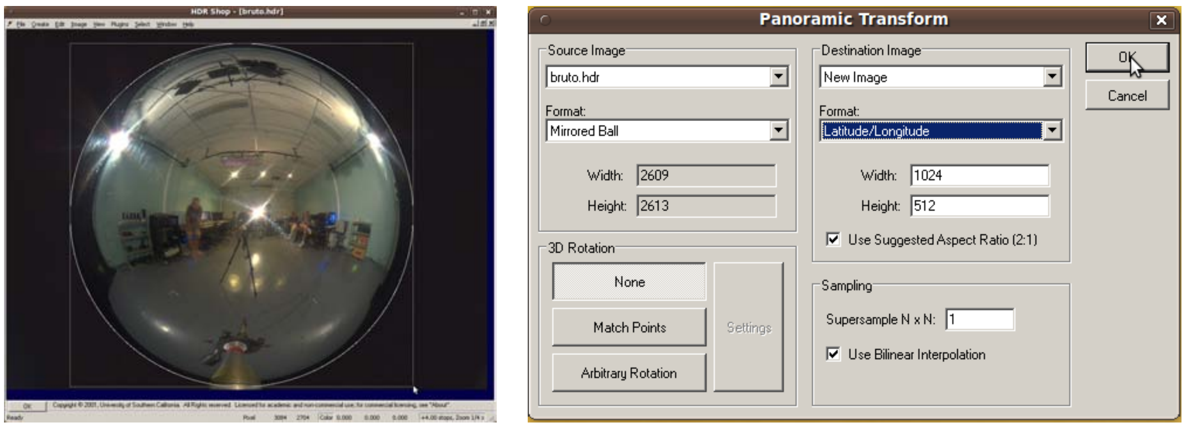

Panoramic Transform

Source Image: bruto.hdr

Format: Mirrored Ball

Width: 2609

Height: 2613

3D Rotation: None | Match Points | Arbitrary Rotation | Settings

Destination Image: New Image

Format: Latitude/Longitude

Width: 1024

Height: 512

☑ Use Suggested Aspect Ratio (2:1)

Sampling

Supersample N x N: 1

☑ Use Bilinear Interpolation

OK | Cancel

(a) (b)

Figure 6.5: (a) Select the mirror ball with the circle option cheked in the crop tool,(b) The panoramic transformation window, used to transform from the Mirrored Ball format to Latitude/Longitude format.

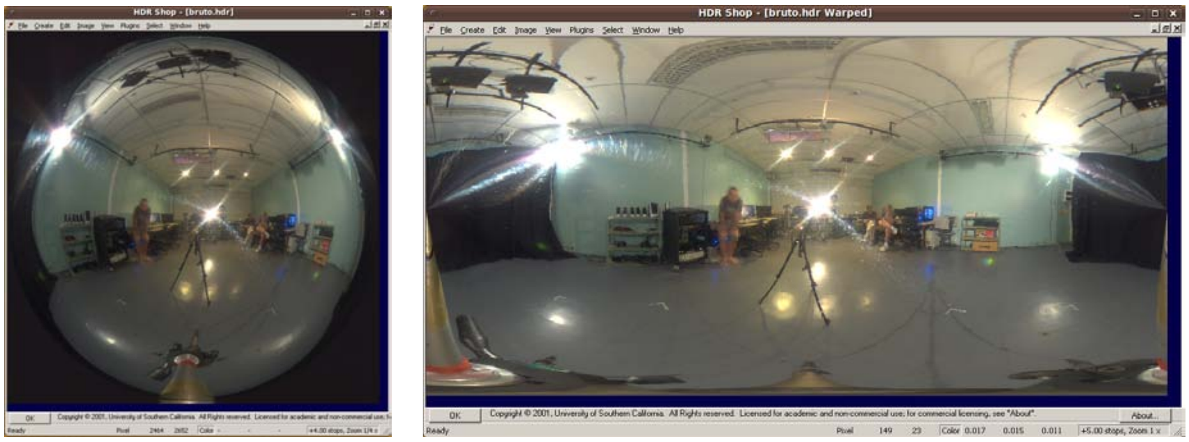

(a) (b)

Figure 6.6: (a) The Light Probe in mirrored format, (b) The Light Probe in Latitude-Longitude format.

Calibrating Sphere reflectivity

We should note that the materials commomly used in mirrored spheres can't reflect the 100% of incident illumination, so the ball used has a coefficient of reflection that we must calculate to correct the obtained illumination map.

To calculate the reflection coefficient of the mirrored ball and fix the map we follow these steps:

- We set a patch on a sheet of white diffuse paper and put it near the mirrored sphere. So we took a picture that contains both the paper and the sphere (figure 6.7).
- We can thus divide the average pixel value of the patch in the reflection by the average pixel value in the direct view to obtain the coefficient of reflection in each color channel. In our case the result is $(0.625460, 0.664949, 0.706071)$.

- The map can be corrected to match the backgroud by dividing its channels by each of these numbers.

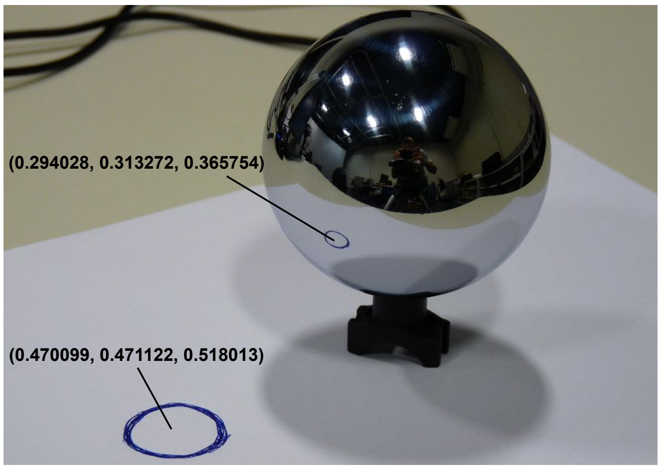

Figure 6.7: The average colors of a white patch in real world and its reflection on the mirrored ball. Dividing these two values you get the reflectivity coefficient of the mirrored ball.

6.3 Rendering with Light Maps in Mental Ray

To open the ilumination map in MAYA and using it in rendering we should follow up this steps:

1. Go to menu **Window→Rendering Editor→Render Settings**. Whitin the **Render Settings** window we do:
    - Mark **Render Using** option as **mental ray** (figure 6.8(a));
    - Uncheck **Enable Default Light** option in **Rendering Options** sections of the **Commom** tab figure 6.8(a));
    - Click in **Create** buton of the **Image based Lightling** option, inside **Environment** section of **mental ray** tab figure 6.8(c)).
2. Inside **mental ray** tab, go to **Rendering Features** section and just check **raytracing** item of **Secondary Effects** option (figure 6.8(b)). It's possible add more effects like caustics, global illumination and final gathering. However this resources will require another scheme to set the illumination map correctly.
3. Go to **Attribute Editor** of the *Image Based Lighting* created before. To access it just clik in the created sphere with the *selection tool.*
    - In **Image Based Lighting Attributes** section, if you click in the icon besided image name field you can explore other files and select the hdr illumination map done in section before (red circle in figure 6.9(a)).

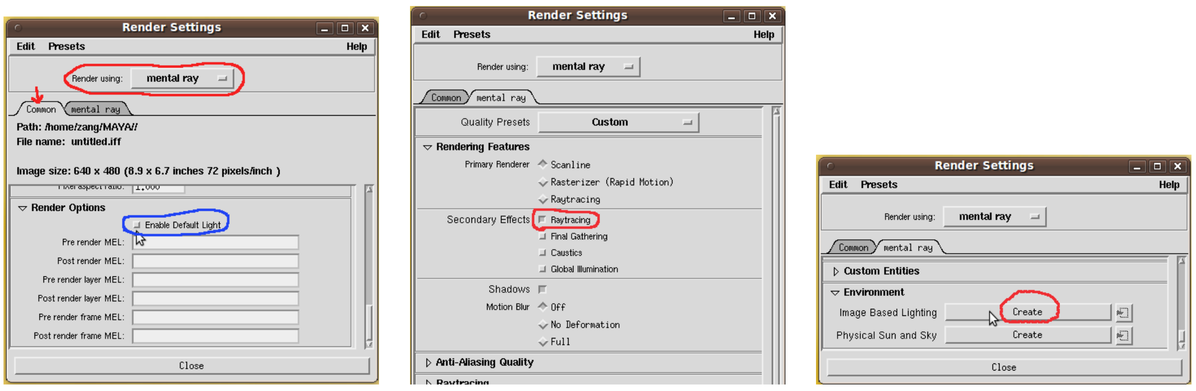

Render using: mental ray

Path: /home/zang/MAYA//
File name: untitled.iff

Image size: 640 x 480 (8.9 x 6.7 inches 72 pixels/inch)

Render Options
Enable Default Light
Pre render MEL:
Post render MEL:
Pre render layer MEL:
Post render layer MEL:
Pre render frame MEL:
Post render frame MEL:

Quality Presets: Custom
Rendering Features
Primary Renderer: Scanline / Rasterizer (Rapid Motion) / Raytracing
Secondary Effects: Raytracing / Final Gathering / Caustics / Global Illumination
Shadows
Motion Blur: Off / No Deformation / Full
Anti-Aliasing Quality
Raytracing

Custom Entities
Environment
Image Based Lighting: Create
Physical Sun and Sky: Create

(a) (b) (c)

Figure 6.8: The Render Settings menu.

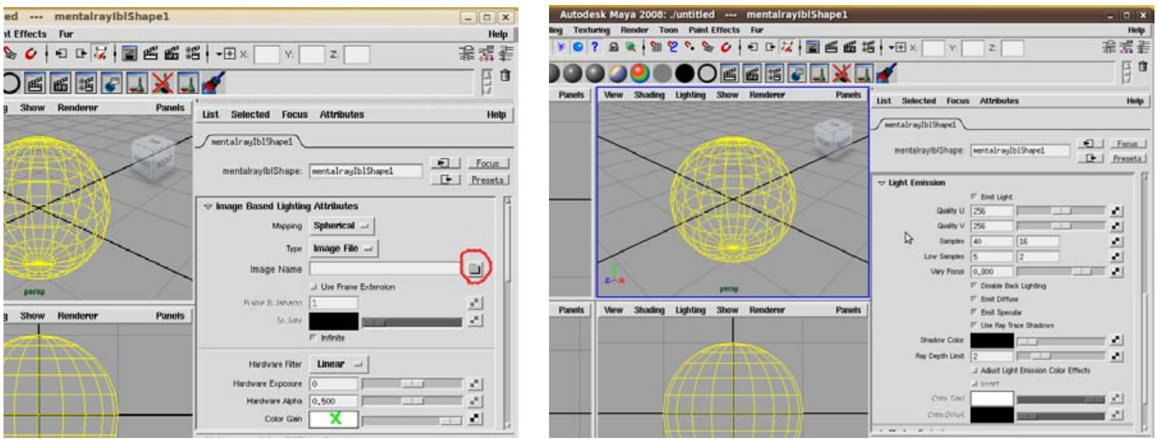
mentalrayIblShape1
Autodesk Maya 2008: ./untitled --- mentalrayIblShape1
List Selected Focus Attributes Help
Show Renderer Panels
View Shading Lighting Show Renderer Panels
Focus
Presets
persp

mentalrayIblShape: mentalrayIblShape1

Image Based Lighting Attributes
Mapping: Spherical
Type: Image File
Image Name
Use Frame Extension
Infinite
Hardware Filter: Linear
Hardware Exposure: 0
Hardware Alpha: 0.500
Color Gain

Light Emission
Emit Light
Quality U: 256
Quality V: 256
Samples: 40 16
Low Samples: 5 2
Vary Focus: 0.000
Disable Back Lighting
Emit Diffuse
Emit Specular
Use Ray Trace Shadows
Shadow Color
Ray Depth Limit: 2
Adjust Light Emission Color Effects

(a) (b)

Figure 6.9: The Attribute Editor of the *Image Based Lighting.*

- If it's necessary you can adjust the map Gain in **Color Gain** option. Clicking in the white rectangle you will open the **Chooser Color** in wich we can choose the color and the gain intesity (green X in figure 6.9(a)). Usually we will maintain white color and just change it intensity, which can be done changing the parameter **V** value (if the color chooser is set as HSV).
- In Light Emission section, check the Emit Light item (figure 6.9(b)). The Quality U and Quality V attributes set the size of a control texture that generates the virtual lights. For each pixel of the ocntrol texture, one light is creted. To make the render feasible, the Samples attribute places a cap of the number of lights used. The first Samples field determines the minimum number of lights generated. The second Samples field determines the maximum number of additional lights that are randomly added to make the lighting less regular. To set these parameters you must consider the desired quality and rendering time.

Chapter 7

Camera Calibration

Camera calibration techniques are methods used for finding the intrinsic and extrinsic parameters of cameras. These methods are very important whenever we intend to superimpose synthetic images over real ones in a realistic way. It holds because the effect applied by the camera model used in the rendering process must correspond to the effect applied by the real camera.

7.1 Introduction

There are two types of methods for calibrating cameras:

- Methods that use correspondences of 3D points to 2D points,
- Methods that use correspondences between 2D points.

The first type uses some kind of 3D pattern, which have markers placed in known positions. Correspondences between these markers and theirs 2D projections over an image are established. Then the method finds a camera model defined relatively to the 3D pattern.

This is a good choice if we want to superimpose a 3D model over a single frame. In this case we take two pictures without moving the camera. One picture must show the 3D pattern in order to be used by the calibration method, the other one does not show the pattern, this is the picture that is superimposed by the 3D model (see Figure 7.1).

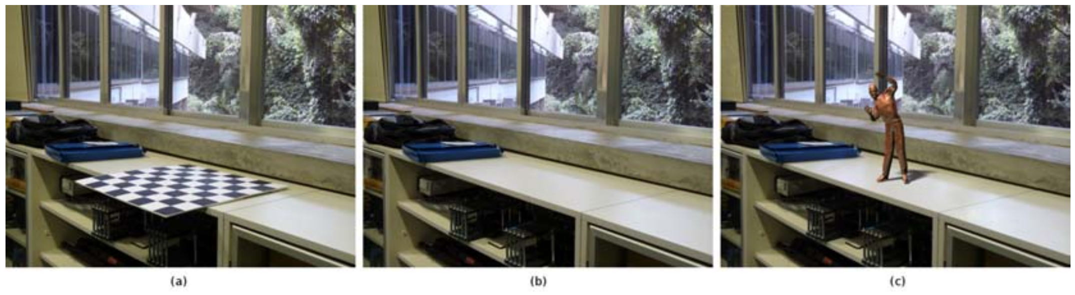

Figure 7.1: (a) The picture of a scene showing a 3D planar pattern, (b) the scene after removing the 3D pattern, (c) a 3D model superimposed to the scene.

The second type is more sophisticated. Correspondences are established between projections of static points over many images using image processing techniques. Then the method finds a camera model associated to each image. It is good because no pattern is needed, but the absence of 3D markers implies that the correspondence of points can easily fail. Thus, robust techniques must be added to the process. This process is called Matchmove by 3d artists. We will not talk about them here, examples of algorithms that do it can be found in [21] and [22].

7.2 Calibration Techniques

There are different algorithms for solving calibration problems based on 3D patterns. The most important are:

Tsai's Algorithm The Tsai's algorithm makes use of a single planar pattern, usually a checkerboard. It is the algorithm used in the Figure 7.1. It is a simple algorithm, but it does not allow us to find all camera parameters. It cannot find the aspect ratio of pixels neither the principal point. In general it is not a big trouble since we usually assume that pixels are squared and the principal point is placed in the center of the image. An implementation of it can be found in `http://www.cs.cmu.edu/~rgw/TsaiCode.html`.

DLT Algorithm The Direct Linear Transformation algorithm solves the problem of calibrating cameras using correspondences of 3D known points to theirs respective projections. Compared to the previous algorithm it consider 3D points in a more unbiased form, since they do not have to be placed over a plane. Another advantage is the fact that it can find all the camera parameters. The disadvantage to Tsai's algorithm is the fact that it needs a non planar pattern, what is in general more difficult to be built with good precision. Details of this algorithm can be found in [23].

Zhang's Algorithm The Zhang's algorithm makes use of a planar pattern that is photographed from many different poses. Like Tsai's algorithm checkerboards are usually used. It combines two good properties from the previous methods. It uses a planar pattern, what is easily built, and the 3D markers are not placed over a plane , what makes the calibration unbiased. An implementation is available in `http://www.vision.caltech.edu/bouguetj/calib_doc/index.html`.

7.3 Calibration and MoCap

In this project we faced a very specific calibration problem. We needed to superimpose a 3D character over the image of a dancer whose movements were being used to animate this character (see Fig 7.2). The solution for this problem is calibrating the camera in the same reference used by the MoCap system.

The first idea that we had was placing markers over a checkerboard and combine the values of rotation and translation given by the MoCap system with the camera parameters estimated by Tsai's or Zhang's algorithm. It would have been complicated, and we were

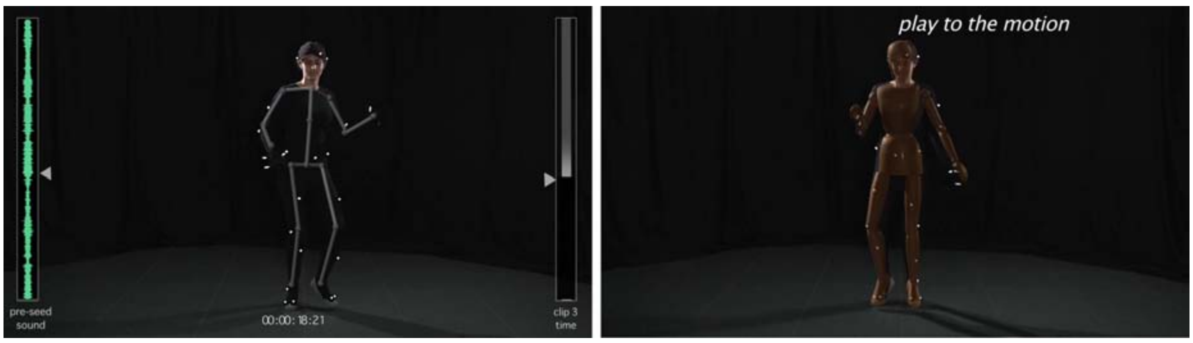

Figure 7.2: 3D characters superimposed to the the dancer.

not completely confident that we were able to interpret the information of translation and rotation given by the Arena software exactly.

We decided to solve it in a more direct way. We took many pictures showing markers used by the MoCap system (see Figure 7.3). For each pose we registered those 3D coordinates given by the MoCap system. After that, we registered the 2D coordinates of each marker using an ordinary image editor. Then we used the DLT algorithm to calibrate the camera using the 3D-2D correspondences established.

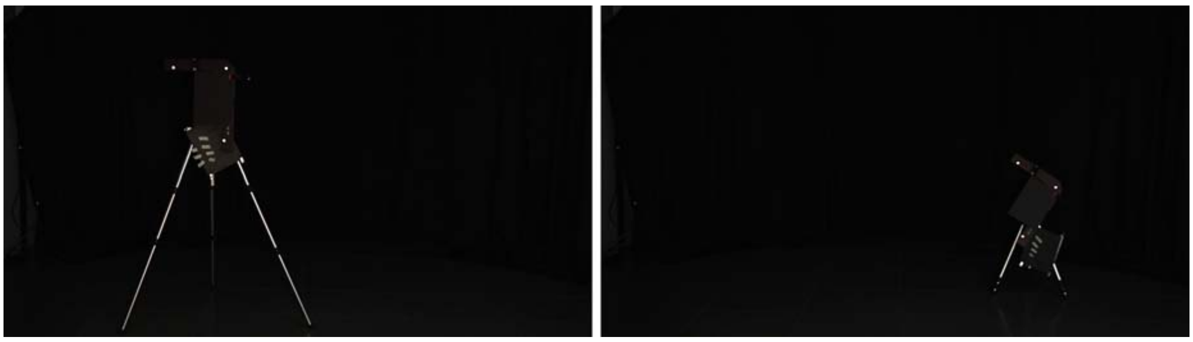

Figure 7.3: Each picture shows three different markers used by the calibration algorithm.

After performing the DLT algorithm we found that the camera is $K[R|t]$ where:

$$K = \begin{pmatrix} -2186 & 0 & 946 \\ 0 & 2191 & 501 \\ 0 & 0 & 1 \end{pmatrix}, \tag{7.1}$$

$$R = \begin{pmatrix} -0.006 & -0.028 & 0.999 \\ -0.091 & 0.995 & 0.027 \\ -0.995 & -0.091 & -0.009 \end{pmatrix} \tag{7.2}$$

and

$$t = \begin{pmatrix} -8.660 & -79.719 & 403.274 \end{pmatrix}^T. \tag{7.3}$$

The extrinsic parameters can be calculated by:

$$CameraCenter = -R^T t = \begin{pmatrix} 394.214 & 115.940 & 14.594 \end{pmatrix}^T, \tag{7.4}$$

$$ViewDirection = R^T\,(0,0,1)^T = \left(\begin{array}{ccc} -0.995 & -0.091 & -0.009 \end{array}\right)^T \tag{7.5}$$

and

$$ViewUp = R^T\,(0,1,0)^T = \left(\begin{array}{ccc} -0.091 & 0.995 & 0.027 \end{array}\right)^T. \tag{7.6}$$

We can set all these parameters in Maya using the following MEL command:

```
viewPlace -eye 394.214 115.940 14.594 -viewDirection -0.995 -0.091 -0.009
                            -up -0.091 0.995 0.027;
```

After setting the position and orientation, we must set the intrinsic parameters. It can be done by changing the attributes of cameraShape. We must adjust the *Focal Length*, the *Camera Aperture* and the *Film Translate* parameters (see Figure 7.4).

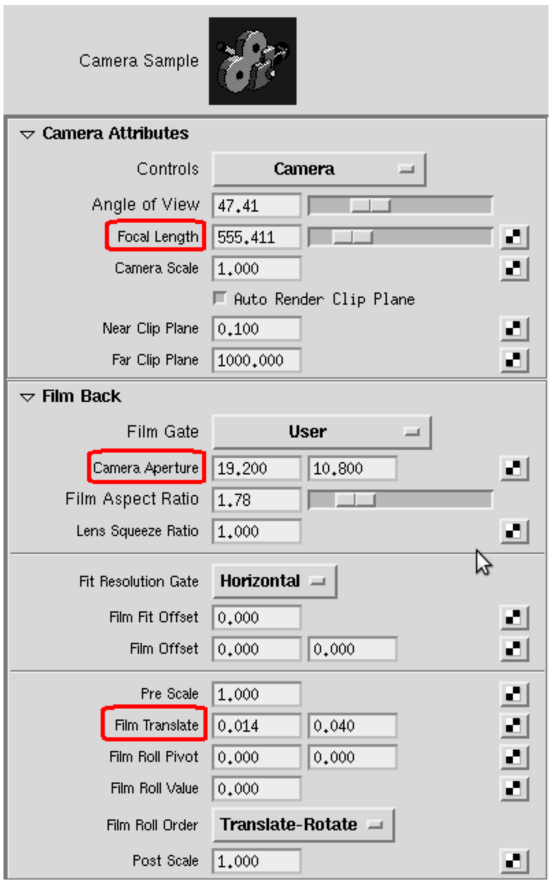

Camera Sample		
Camera Attributes		
Controls	**Camera**	
Angle of View	47.41	
Focal Length	555.411	
Camera Scale	1.000	
	Auto Render Clip Plane	
Near Clip Plane	0.100	
Far Clip Plane	1000.000	
Film Back		
Film Gate	**User**	
Camera Aperture	19.200	10.800
Film Aspect Ratio	1.78	
Lens Squeeze Ratio	1.000	
Fit Resolution Gate	**Horizontal**	
Film Fit Offset	0.000	
Film Offset	0.000	0.000
Pre Scale	1.000	
Film Translate	0.014	0.040
Film Roll Pivot	0.000	0.000
Film Roll Value	0.000	
Film Roll Order	**Translate-Rotate**	
Post Scale	1.000	

Figure 7.4: CameraShape attributes. *Focal Length*, *Camera Aperture* and *Film Translate* are marked.

The *Focal Length* and the *Camera Aperture* are related, if we multiply both by the same scalar factor the result is an equivalent camera. This fact is very important because Maya only accepts focal lengths from 2.5” to 3500”. Thus we must choose a factor that give us an acceptable value. Another issue is that the *Focal Length* is specified in inches, but the *Camera Aperture* field is specified in mm. The expressions to calculate them are:

$$FocalLength = -25.4 \times K_{11} \times ScaleFactor$$

$$HorizontalCameraAperture = ResX \times ScaleFactor$$

$$VerticalCameraAperture = ResY \times ScaleFactor$$

,where K is the matrix of intrinsic parameters and ResX and ResY are the horizontal and vertical image resolution respectively.

In our example we chose 0,01 as the scalar factor, what results in:

$$FocalLength = 555.41''$$

$$HorizontalCameraAperture = 19.2mm$$

$$VerticalCameraAperture = 10.8mm.$$

Film Translate is the parameter that encodes the principal point coordinates. They are the coordinates measured in pixels of the point where the view direction crosses the image plane. Maya assumes, as default, that the principal point is placed in the middle of the image, in the case of an image with resolution 1920×1080 it would be $(950, 540)^T$. On the other hand, we can read the principal point associated to our camera reading the two top right values of the matrix K in 7.1, which give us $(946, 501)^T$. The difference between the calibrated coordinates and the center of the image must be encoded in the *Film Translate* parameter. The following expressions adjust the values to what Maya expects:

$$HorizontalFilmTranslate = \frac{(ResX/2 - K_{13})}{ResX/2}$$

$$VerticalFilmTranslate = \frac{(ResY/2 - K_{23})}{ResX/2}$$

Considering our example it results in:

$$HorizontalFilmTranslate = 0.014$$

$$VerticalFilmTranslate = 0.040$$

After setting all the parameters we can check if the camera is correct. Looking throw the camera, the projection of 3D points whose vertices had been used by the calibration process must match the image of these points in a image plane assigned to the camera (see Figure 7.5).

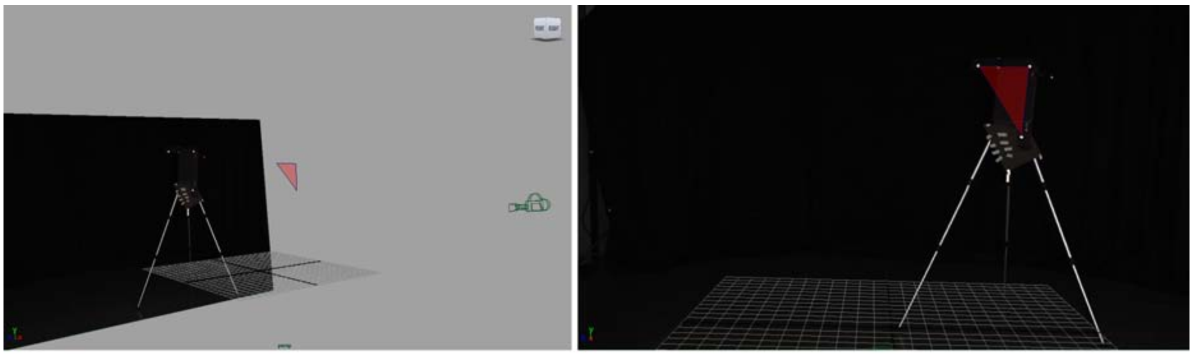

Figure 7.5: The 2D projections of 3D points match the projection in the picture used as image plane.

Chapter 8

Music

In this chapter we will describe the *motion scoring* procedure, ie, the pipeline for music composition. There are five steps:

1. Some songs are composed.
2. A dancer performs listening to the songs, and the dance is captured.
3. A graph of the dancer's motion (*coreo.graph*) is built.
4. A new motion is synthesized by random-walking on the *coreo.graph*.
5. A new song, based on the walk on the graph, is composed.

8.1 Automatic Composition

We have chose to compose songs in the brazilian *samba* style, specially because of its simplicity regarding the number os musical instruments to use and the complexity of implementing tracks for them. Essentially, we need just an instrument for each one of the percussion, harmony and melody categories. In samba, *cavaquinho* and *pandeiro* (in english, tambourine) are classically used for harmony and percussion, respectively. Regarding melody, there is the cavaquinho, the flute, the mandolin and other choices (like the human voice, for instance).

As everything else in music, there is no rigorous rule for composing a samba song, and in fact we are not experts in the subject. That said, given the human build-in capability to produce music, some knowledge we have about music theory and a little bit of previous experience we brought from other styles, it's not too difficult to become capable of composing samba songs after hearing a couple of samples, talking to a friend which likes samba and, of course, taking some video lessons on YouTube.

We have composed three music pieces to be performed by the dancer. Each music is organized in a 4-levels multi-resolution structure, consisting of *cycles*, *bars* (measures), *beats* and *clocks*: 16 bars per cycle, 2 beats per bar and 12 clocks per beat.

For each song we have varied the melodic instrument, using the flute, the cavaquinho and the clarinet. All songs were composed to have 3 cycles, the second (resp. first) being the more (resp. the less) musically intense. "Intensity" of a song is a highly subjective concept, but we can simulate it reasonably by putting intensity in direct proportion with the number of notes per bar which are played. The presence or not of a percussion instrument affects music intensity as well.

Drum loops (ie, pandeiro loops) were composed manually, as well as cavaquinho loops. We have chosen to use G, E7, Am, D7 as the chord progression. The melody is organized in phrases, each phrase extending a bar (measure). Notes for each phrase are not picked manually. Instead, we specify just the *number of notes* that must be played for each one of the (two) beats of the phrase.

Beats can be filled with 0, 1, 2, 3, 4 or 6 equally spaced notes, what explains why we are using 12 clocks as the resolution for the beat. This way, composing for a phrase means calling a functions saying something like:

```
fill beat 1 with m notes,
fill beat 2 with n notes.
```

In fact sometimes another slightly different method is called:

```
fill beat j with m notes, the first note being of type x.
```

The type of the note has to do with the current chord being played, but we will not get into the details (which are related to music theory concepts). This extra restriction is usually observed in the first beat of the measure, because, in our implementation, that is when the chord of the harmony is changing (there is a chord change every new bar).

In the particular implementation used for this project, for the

```
fill beat j with m notes
```

method the new note is simply one step above or bellow the chosen musical scale (which, by the way, is the diatonic major), while for the method

```
fill beat j with m notes, the first note being of type x
```

the algorithm skips up or down the scale until a note which "sounds good" with the current chord is reached.

If the algorithm will search for a note up or down the scale is a matter of

- a random sample taken from a uniform distribution in the interval $[0, 1]$ being greater or smaller than $1/2$ and

- a note in the chosen direction being available.

Notes are confined in a 4×9 grid, as shown in Figure 8.1. The distribution of the diatonic scale notes in the grid are described in [24].

Since in the grid the same musical note can be associated with more than one point, the algorithm decides which point to use by, again, tossing a fair coin.

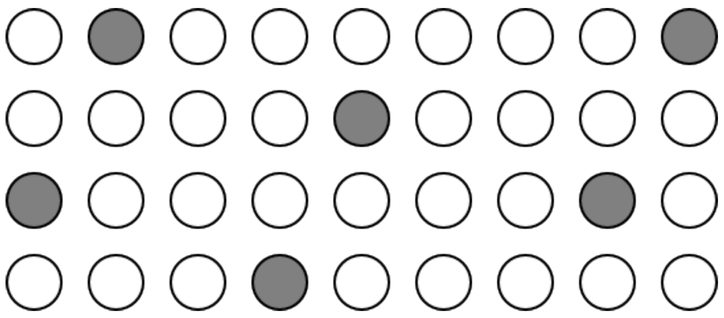

Figure 8.1: Grid of notes for the automatic composition. Gray filled circles represent scale-root notes.

8.2 Motion Scoring

After the songs are composed, the dancer performs listening to them. As mentioned in Chapter 4, the captured motion of the dancer is segmented according to the length of a musical phrase, which is equal to the length of a measure (bar), as described in the previous section. That is why the motion graph so built is said to be *measure-synchronous*. Once a new dance is obtained by random-walking on such a graph (the *choreo.graph*), the next step is to compose the music score for it.

Let us suppose that we have constructed a new dance consisting of 4 segments,

`(c1|s4), (c3|s12), (c3|s13), (c2|s10),`

where `(cI|sJ)` means the segment `J` of clip (song) `I`. Now let us say that `(c1|s4)` was composed using the high-level command:

```
fill beat 1 with 4 notes, the first note being of type x
                  fill beat 2 with 2 notes
```

and that the tambourine was omitted in that phrase. Then the first phrase of the score for the re-synthesized dance will be composed the same way: the first beat will be filled with 4 notes, the first of which being of type `x`, the second beat will be filled with 2 notes, and the percussion will be omitted.

The chord progression can be set manually, or we can simply use the same sequence of chords for the pre-dance songs and for the re-synthesized dance.

Chapter 9

Motion Graphics

The graphics in the video were created for the opening title sequence and to annotate the live perfomance clip as well as the cg animation generated by the dance graph.

9.1 Opening Title

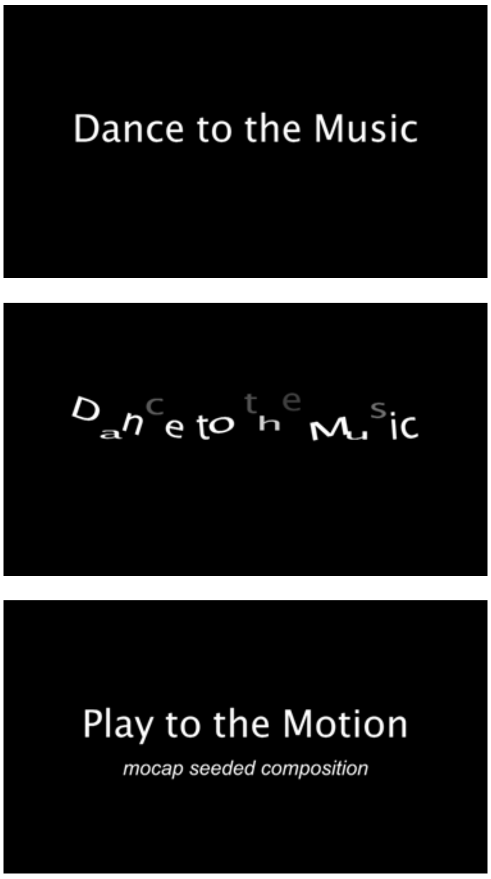

Figure 9.1: Opening Title

The opening title, shown in Figure 9.1, was produced using the Live Type software, part of the Final Cut Studio, from Apple.

9.2 Live Action Clip

The live action dance performance in the first part of the video was annotated with superimposed graphical elements created with the program After Effects, from Adobe. (See Figure 9.2)

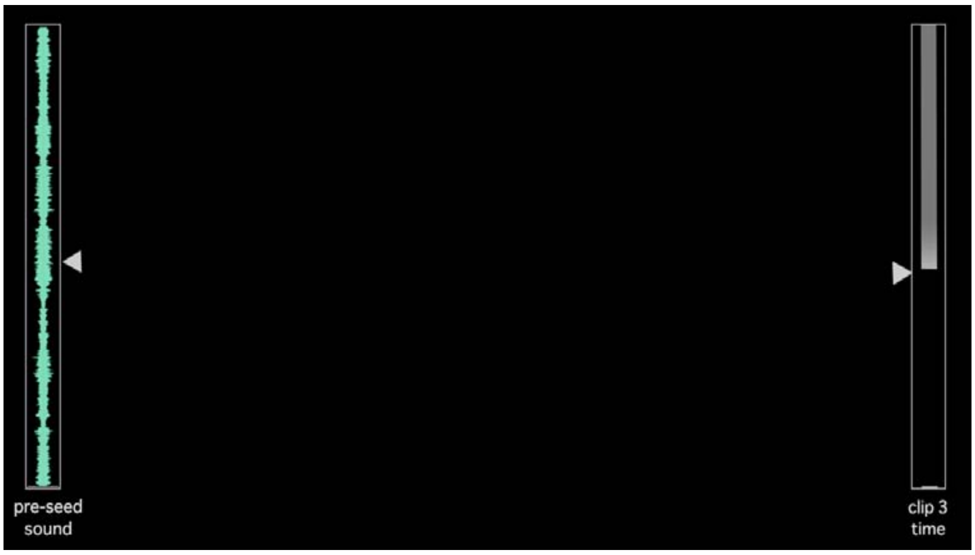

Figure 9.2: Live Performance Annotations.

9.3 Dance Graph

The computer generated animation in the second part of the video was annotated with a graphical layer that showed the progression of the dance graph. This effect was generated by a custom program developed using the Apple Quartz graphics. (See Figure 9.3)

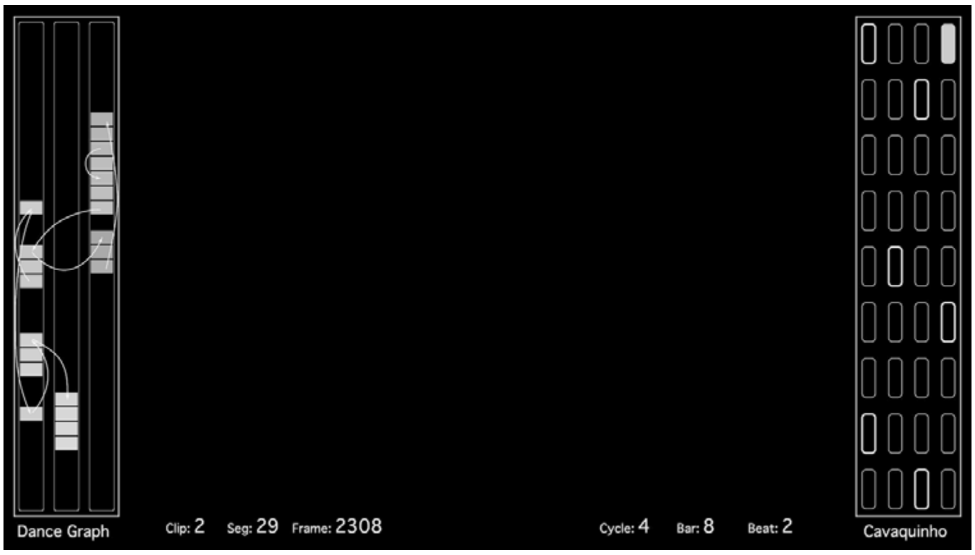

Figure 9.3: Dance Graph Annotations.

Appendix A

BVH File Format

In this Appendix We will describe the BVH file format by means of a simple example. Consider the following BVH file:

```
HIERARCHY
ROOT A
{
    OFFSET 0.000000 0.000000 0.000000
    CHANNELS 6 Xposition Yposition Zposition Zrotation Xrotation Yrotation
    JOINT B
    {
        OFFSET 10.000000 0.000000 0.000000
        CHANNELS 3 Zrotation Xrotation Yrotation
        End Site
        {
            OFFSET 0.000000 -20.000000 0.000000
        }
    }
}

MOTION
Frames:    3
Frame Time:    0.040000
30.0    80.0    20.0    0.0     0.0     0.0      0.0    0.0    0.0
30.0    80.0    20.0    60.0    0.0     0.0      0.0    0.0    0.0
30.0    80.0    20.0    60.0    0.0     0.0    -30.0    0.0    0.0
```

The first part of the file describes the skeleton, which has a root node A, a joint B and and ending node C, as illustrated in Figure A.1. Notice that the the distance between the nodes are given by the offsets described in the file. In this example $O_A = [0\ 0\ 0]$, $O_B = [10\ 0\ 0]$, and $O_C = [0\ -20\ 0]$.

This part of the file also details the channels associated to each node and therefore indicates the size of the motion data and what is the information of each entry of the motion vector. In this case, node A has 6 channels and node B, 3 channels. This means

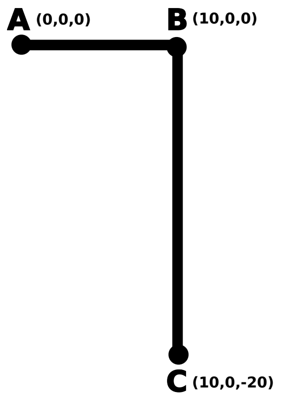

Figure A.1: Articulated body.

that the motion data (second part of the file) will be a series of vectors of size 9, each corresponding to a single frame.

Consider, for example, the third frame (third line of the file after `MOTION`). The first three components are the translation of node A ($T_A = [30\ 80\ 20]$), the second three are the rotations associated to this node, R_A, and the last three are the rotations associated to node B, R_B. Notice that the order of rotations are given in the first part of the file. In this example we first rotate 60^o around the z axis, than 0^o around the x axis, and, finally, the 0^o around the y axis. Therefore, $R = R_y R_x R_z$.

Finally, we calculate the position of each node using the following equations:

$$\begin{cases} A = O_A + T_A \\ B = A + O_b R_A \\ C = B + O_c R_B R_A \end{cases}$$

Figure A.2 illustrates the arm position in frames 2 and 3.

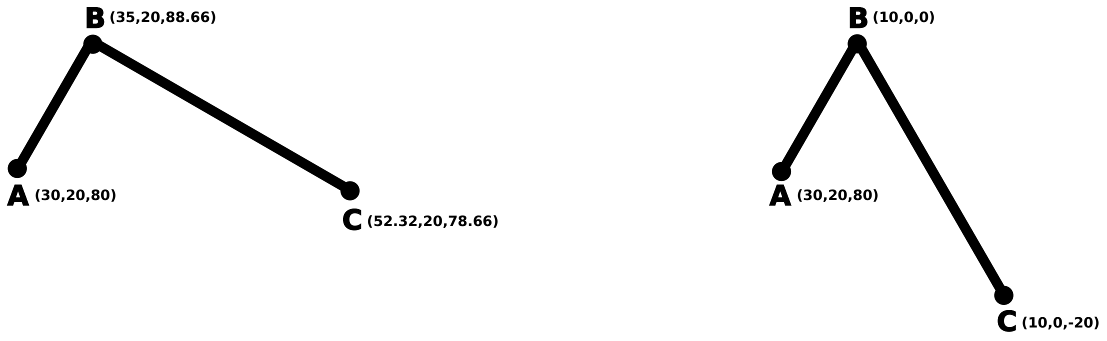

(a) Frame 2 (b) Frame 3

Figure A.2: Articulated body motion.

Bibliography

[1] Chris Bregler. Motion capture technology for entertainment [in the spotlight]. *Signal Processing Magazine, IEEE*, 24(6):160–158, November 2007.

[2] Jessica Hodgins and Zoran Popovic. *Animating Humans by Combining Simulation and Motion Capture*. SIGGRAPH'00 Course Notes 33, SIGGRAPH-ACM publication, New Orleans, Louisiana, USA, July 2000.

[3] Michael Gleicher. Animation from observation: Motion capture and motion editing. *SIGGRAPH Comput. Graph.*, 33(4):51–54, 2000.

[4] Jessica Hodgins. Animating human motion. *Scientific American*, 278(3), March 1998.

[5] Charlotte Belland, James W. Davis, Michael Gleicher, and Barbara Helfer. *Motion Capture: Pipeline, Applications, and Use*. SIGGRAPH'02 Course Notes 28, SIGGRAPH-ACM publication, San Antonio, Texas, USA, July 2002.

[6] Rick Parent. *Computer animation: algorithms and techniques*. Morgan Kaufmann Publishers Inc., San Francisco, CA, USA, 2002.

[7] Margaret S. Geroch. Motion capture for the rest of us. *J. Comput. Small Coll.*, 19(3):157–164, 2004.

[8] Maureen Furniss. *Motion Capture*. MIT Communications Forum, http://web.mit.edu/comm-forum/papers/furniss.html.

[9] Andrew Witkin and Zoran Popovic. Motion warping. In *SIGGRAPH '95: Proceedings of the 22nd annual conference on Computer graphics and interactive techniques*, pages 105–108, New York, NY, USA, 1995. ACM.

[10] Armin Bruderlin and Lance Williams. Motion signal processing. In *SIGGRAPH '95: Proceedings of the 22nd annual conference on Computer graphics and interactive techniques*, pages 97–104, New York, NY, USA, 1995. ACM.

[11] Yan Li, Tianshu Wang, and Heung-Yeung Shum. Motion texture: a two-level statistical model for character motion synthesis. In *SIGGRAPH '02: Proceedings of the 29th annual conference on Computer graphics and interactive techniques*, pages 465–472, New York, NY, USA, 2002. ACM.

[12] Matthew Brand and Aaron Hertzmann. Style machines. In *SIGGRAPH '00: Proceedings of the 27th annual conference on Computer graphics and interactive techniques*, pages 183–192, New York, NY, USA, 2000. ACM Press/Addison-Wesley Publishing Co.

[13] Lucas Kovar and Michael Gleicher. Automated extraction and parameterization of motions in large data sets. *ACM Trans. Graph.*, 23(3):559–568, 2004.

[14] Lucas Kovar, Michael Gleicher, and Frédéric Pighin. Motion graphs. In *SIGGRAPH '02: Proceedings of the 29th annual conference on Computer graphics and interactive techniques*, pages 473–482, New York, NY, USA, 2002. ACM.

[15] Autodesk Maya Press. *Getting Started with Maya 7*. 2005.

[16] Autodesk Maya Press. *Learning Autodesk Maya 2009 The Modeling & Animation Handbook: Official Autodesk Training Guide (Autodesk Maya Techniques Offical Autodesk Training Guides)*. SYBEX Inc., Alameda, CA, USA, 2008.

[17] Eric Allen and Kelly L. Murdock. *Body Language: Advanced 3D Character Rigging*. SYBEX Inc., Alameda, CA, USA, 2008.

[18] Lee Lanier. *ADVANCED MAYA - TEXTURING AND LIGHTING 2nd Edition*. SYBEX Inc., Alameda, CA, USA, 2008.

[19] Paul Debevec. Rendering synthetic objects into real scenes: Bridging traditional and image-based graphics with global illumination and high dynamic range photography. In *SIGGRAPH*, pages 189–198, 1998.

[20] Paul Debevec and Jitendra Malik. Recovering high dynamic range radiance maps from photographs. In *SIGGRAPH*, pages 369–378, 1997.

[21] Bruno Madeira, Luiz Velho, and Paulo Cezar Carvalho. Calibracao robusta de video para realidade aumentada. In *Proceedings of IX Symposium on Virtual and Augmented Reality*. SBC, 2007.

[22] J. Cook T.L.J. Howard R. J. Hubbold S. Gibson and D. Oram. Accurate camera calibration for off-line, video-based augmented reality. In *International Symposium on Mixed and Augmented Reality (ISMAR 2002)*. IEEE and ACM, 2002.

[23] R. I. Hartley and A. Zisserman. *Multiple View Geometry in Computer Vision*. Cambridge University Press, ISBN: 0521540518, second edition, 2004.

[24] Marcelo Cicconet, Tertuliano Franco, and Paulo Cezar Carvalho. Plane tessellation with musical scale tiles and bidimensional automatic composition. In *International Computer Music Conference*, 2010.